Electronic Supporting Information

Ethylene carbonate splitting and Claisen-type self-addition of *γ*-butyrolactone promoted by an oxygen-bridged Ga/P FLP

Julian Buth,[a] Beate Neumann,[a] Jan-Hendrik Lamm,[a] Hans-Georg Stammler,[a] Yury V. Vishnevskiy,[a,b] and Norbert W. Mitzel*[a]

[a]Lehrstuhl für Anorganische Chemie und Strukturchemie, Centrum für Molekulare Materialen CM_2, Fakultät für Chemie, Universität Bielefeld, Universitätsstraße 25, Bielefeld 33615, Germany.
E-mail: mitzel@uni-bielefeld.de

[b]Department of Chemistry, M. V. Lomonosov Moscow State University, Leninskie Gory 1–3, Moscow 119991, Russia

Table of content

1) Experimental details

General methods

All reactions and manipulations with air and moisture sensitive compounds were carried out under conventional Schlenk techniques or in a glove box using argon as inert gas. Volatile compounds were handled in a vacuum line. The solvents *n*-hexane, toluene, toluene-d_8 and benzene-d_6 were dried over a Na/K alloy, distilled and degassed prior to use. $Bis_2Ga–O–P^tBu_2$ (**GaOP**) was prepared according to literature procedure.[36] Benzaldehyde, cyclopentanone (CP), *γ*-butyrolactone (GBL), propylene oxide (PO), phenylacetylene, trimethylsilyl acetylene and benzyl chloride were degassed, dried over mole sieves (4 Å) and distilled prior to use. Ethylene carbonate (EC) was used without further purification. NMR spectra were recorded using a Bruker Avance III 500, Avance III 500 HD, Ascend 500 neo2K or Ascend 500 neo3K spectrometer at ambient temperature unless otherwise stated. Chemical shifts were referenced to the residual proton or carbon signal of the solvent (benzene-d_6: ^{1}H: 7.16 ppm, ^{13}C: 128.1 ppm; toluene-d_8: ^{1}H: 2.09 ppm) or externally (^{29}Si: $SiMe_4$, ^{31}P: 85% H_3PO_4 in H_2O). Elemental analyses were carried out using a HEKATECH EURO Elemental Analyzer.

Synthetic procedure

$Bis_2Ga–O–P^tBu_2$ (**GaOP**) was dissolved in toluene (2 mL), the substrate was added and the reaction was stirred for 24 h at room temperature, unless otherwise stated. All volatiles were removed under reduced pressure and the residue dried in *vacuo*.

$Bis_2Ga–O–P^tBu_2$·PhCHO (**1**): Using benzaldehyde (5 µL, 4.8 mg, 45 µmol, 1.2 equiv.) and after an additional washing step with *n*-hexane, **1** was obtained as a colourless solid (24 mg, 37 µmol, 97%). ^{1}H NMR (500 MHz, C_6D_6): δ [ppm] = −0.48 (s, 1H, GaC**H**), −0.26 (s, 1H, GaC**H**), 0.36 – 0.58 (m, 36H, Si(C**H**$_3$)$_3$), 0.84 (d, $^3J_{P,H}$ = 13.4 Hz, 9H, C(C**H**$_3$)$_3$), 1.15 (d, $^3J_{P,H}$ = 13.3 Hz, 9H, C(C**H**$_3$)$_3$), 5.85 (s, C**H**O), 7.02 (t, $^3J_{H,H}$ = 7.2 Hz, 1H, *para*-**H**), 7.14 (t, $^3J_{H,H}$ = 7.3 Hz, 2H, *meta*-**H**), 7.72 (d, $^3J_{H,H}$ = 7.6 Hz, 2H, *ortho*-**H**). ^{13}C{^{1}H} NMR (126 MHz, C_6D_6): δ [ppm] = 3.9 (s, Si(**C**H$_3$)$_3$), 4.6(s, Si(**C**H$_3$)$_3$), 4.6 (s, Si(**C**H$_3$)$_3$), 4.8 (s, Si(**C**H$_3$)$_3$), 6.6 (s, Ga**C**H), 27.1 (s, C(**C**H$_3$)$_3$), 28.2 (s, C(**C**H$_3$)$_3$), 35.3 (s, **C**(CH$_3$)$_3$), 37.0 (s, **C**(CH$_3$)$_3$), 75.5 (d, $^1J_{P,C}$ = 40.4 Hz, **C**HO), 126.3 (s, *ortho*-**C**), 127.2 (s, *para*-**C**), 128.3 (s, *meta*-**C**), 141.6 (s, *ipso*-**C**). ^{29}Si{^{1}H} NMR (99 MHz, C_6D_6): δ [ppm] = −1.1 (s). ^{31}P{^{1}H} NMR (202 MHz, C_6D_6): δ [ppm] = 70.9 (s). Elemental analysis calcd (%) for $C_{29}H_{62}GaO_2PSi_4$ (M_r = 655.85): C 53.11, H 9.53; found C 53.57, H 9.54.

$Bis_2Ga–O–P^tBu_2$·CP (**2**): Using cyclopentanone (10 µL, 9.5 mg, 113 µmol, 1.2 equiv.) and after an additional washing step with *n*-hexane, **2** was obtained as a colourless solid (58 mg, 91 µmol, 93%). ^{1}H NMR (500 MHz, C_6D_6): δ [ppm] = −0.62 (s, 1H, GaC**H**), −0.39 (s, 1H, GaC**H**), 0.42 – 0.50 (s, 36H, Si(C**H**$_3$)$_3$), 0.99 (d, $^3J_{P,H}$ = 13.0 Hz, 9H, C(C**H**$_3$)$_3$), 1.11 (d, $^3J_{P,H}$ = 13.3 Hz, 9H, C(C**H**$_3$)$_3$), 1.48(m, 2H, C**H**$_2$), 1.66 (m, 2H, C**H**$_2$), 2.03 (m, 4H, C**H**$_2$). ^{13}C{^{1}H} NMR (126 MHz, C_6D_6): δ [ppm] = 5.3 (s, Si(**C**H$_3$)$_3$), 6.8 (s, Ga**C**H), 9.9 (s, Ga**C**H), 23.5 (d, $^2J_{P,C}$ = 11.9 Hz, **C**H$_2$), 23.8 (d, $^2J_{P,C}$ = 12.4 Hz, **C**H$_2$), 28.2 (s, C(**C**H$_3$)$_3$), 28.8 (s, C(**C**H$_3$)$_3$), 35.8 (d, $^1J_{P,C}$ = 41.4 Hz, **C**(CH$_3$)$_3$), 37.5 (d, $^1J_{P,C}$ = 41.8 Hz, **C**(CH$_3$)$_3$), 41.1 (s, **C**H$_2$), 42.5 (s, **C**H$_2$), 87.0 (d, $^1J_{P,C}$ = 40.0 Hz,

P**C**O). ^{29}Si{^{1}H} NMR (99 MHz, C_6D_6): δ [ppm] = –1.2 (s). ^{31}P{^{1}H} NMR (202 MHz, C_6D_6): δ [ppm] = 77.2 (s). Elemental analysis calcd (%) for $C_{27}H_{64}GaO_2PSi_4$ (M_r = 633.84): C 51.16, H 10.18; found C 50.78, H 10.14.

Bis$_2$Ga–O–P^{t}Bu$_2$·GBL (**3**): Using *γ*-butyrolactone (10 µL, 11.3 mg, 131 µmol, 1.0 equiv.) and after an additional washing step with *n*-hexane, **3** was obtained as a colourless solid (70 mg, 110 µmol, 87%). ^{1}H NMR (500 MHz, C_6D_6): δ [ppm] = –0.38 (br. s, 1H, GaC**H**), –0.20 (br. s, 1H, GaC**H**), 0.45 (s, 36H, Si(C**H**$_3$)$_3$), 1.10 (m, 18H, C(C**H**$_3$)$_3$), 1.44 (m, 1H, C**H**$_2$), 1.60 (br. m, 1H, C**H**$_2$), 1.93 (br. s, 1H, C**H**$_2$), 2.11 (br. s, 1H, C**H**$_2$), 3.32 (br. s, 1H, C**H**$_2$), 4.00 (br. s, 1H, C**H**$_2$). ^{13}C{^{1}H} NMR (126 MHz, C_6D_6): δ [ppm] = 5.1 (s, Si(**C**H$_3$)$_3$), 9.2 (s, Ga**C**H), 24.7 (s, **C**H$_2$), 27.8 (s, C(**C**H$_3$)$_3$), 35.6 (d, $^{1}J_{P,C}$ = 47.5 Hz, **C**(CH$_3$)$_3$), 36.4 (d, $^{1}J_{P,C}$ = 48.5 Hz, **C**(CH$_3$)$_3$), 39.6 (s, **C**H$_2$), 67.1 (s, O**C**H$_2$), 109.9 (d, $^{1}J_{P,C}$ = 73.2 Hz, P**C**O$_2$). ^{29}Si{^{1}H} NMR (99 MHz, C_6D_6): δ [ppm] = –1.5 (s). ^{31}P{^{1}H} NMR (202 MHz, C_6D_6): δ [ppm] = 74.1 (s). Elemental analysis calcd (%) for $C_{26}H_{62}GaO_3PSi_4$ (M_r = 635.82): C 49.12, H 9.83; found C 48.61, H 10.23.

Bis$_2$Ga–O–P^{t}Bu$_2$·EC (**4**):Using ethylene carbonate (9.1 mg, 103 µmol, 1.1 equiv.) and after an additional washing step with *n*-hexane, **4** was obtained in a colourless, resinlike form (52 mg, 82 µmol, 90%). ^{1}H NMR (500 MHz, C_6D_6): δ [ppm] = –0.30 (br. s, 2H, GaC**H**), 0.45 (s, 36H, Si(C**H**$_3$)$_3$), 1.19 (m, 18H, C(C**H**$_3$)$_3$), 3.28 (br. s, 2H, C**H**$_2$), 3.80 (br. s, 2H, C**H**$_2$). ^{13}C{^{1}H} NMR (126 MHz, C_6D_6): δ [ppm] = 4.9 (s, Si(**C**H$_3$)$_3$), 9.0 (s, Ga**C**H), 27.5 (s, C(**C**H$_3$)$_3$), 35.8 (br. m, **C**(CH$_3$)$_3$), 63.4 (s, O**C**H$_2$), 122.7 (d, $^{1}J_{P,C}$ = 120.4 Hz, P**C**O$_3$). ^{29}Si{^{1}H} NMR (99 MHz, C_6D_6): δ [ppm] = –1.3 (s). ^{31}P{^{1}H} NMR (202 MHz, C_6D_6): δ [ppm] = 70.6 (s). Elemental analysis calcd (%) for $C_{25}H_{60}GaO_4PSi_4$ (M_r = 637.79): C 47.08, H 9.48; found C 46.99, H 9.56.

Claisen addition ring-opening FLP adduct 5: Heating a solution of **GaOP** (55.7 mg, 101 µmol) and GBL (7.9 µL, 8.9 mg ,104 µmol, 1.0 equiv.) in toluene (3 mL) to 70 °C for 6 h, full conversion of the FLP to **5** was observed. After removing all volatiles in *vacuo*, and an additional washing step with *n*-hexane, **5** was obtained in a resin-like form (59.4 mg, 47 µmol, 92%). ^{1}H NMR (500 MHz, C_6D_6): δ [ppm] = –0.48 (s, 2H, GaC**H**), –0.30 (s, 2H, GaC**H**), 0.34 (s, 36H, Si(C**H**$_3$)$_3$), 0.34 (s, 18H, Si(C**H**$_3$)$_3$), 0.36 (s, 18H, Si(C**H**$_3$)$_3$), 0.99 (d, $^{3}J_{P,H}$ = 15.0 Hz, 18H, C(C**H**$_3$)$_3$), 2.10 (tt, *J* = 11.9, 5.8 Hz, 2H, C**H**), 2.49 (m, 2H, C**H**), 2.49 (t, *J* = 8.3 Hz, 2H, C**H**), 3.68 (t, *J* = 8.2 Hz, 2H, C**H**), 4.07 (t, *J* = 6.0 Hz, 2H, C**H**$_2$). ^{13}C{^{1}H} NMR (126 MHz, C_6D_6): δ [ppm] = 3.9/4.1/4.5 (s, Si(**C**H$_3$)$_3$), 7.5/10.3 (s, Ga**C**H), 25.8 (s, C(**C**H$_3$)$_3$), 26.0 (s, **C**H$_2$), 30.9 (s, **C**H$_2$), 33.6 (d, $^{1}J_{P,C}$ = 59.0 Hz, **C**(CH$_3$)$_3$), 36.1 (s, **C**H$_2$), 65.7 (s, O**C**H$_2$), 67.8 (s, O**C**H$_2$), 90.7 (s, **C**CO$_2$Ga), 178.7 (s, **C**O$_2$Ga), 188.0 (s, **C**=O). ^{29}Si{^{1}H} NMR (99 MHz, C_6D_6): δ [ppm] = –1.4 (s), –0.5 (s), –0.3 (s).

Bis$_2$Ga–O–P^{t}Bu$_2$·EO (**7**): After heating a solution of **GaOP** (60.5 mg, 110 µmol) and EC (9.6 mg, 110 µmol, 1.0 equiv.) in toluene (3 mL) to 70 °C for 6 h, full conversion of the FLP to a mixture of Bis$_2$Ga–O–P^{t}Bu$_2$·CO$_2$ (**6**) and **7** was observed. The chemical shifts of **6** are in accordance with the literature values.[34] Crystals of **7**, suitable for X-ray diffraction experiments, were obtained by slow evaporation of a solution in C_6D_6. ^{1}H NMR (500 MHz, C_6D_6): δ [ppm] = –0.40 (br. s, 2H, GaC**H**), 0.49 (s, 36H, Si(C**H**$_3$)$_3$), 0.87 (d, $^{3}J_{P,H}$ = 14.0 Hz, 18H, C(C**H**$_3$)$_3$), 4.10 (dt, $^{3}J_{P,H}$ = 18.5 Hz, $^{3}J_{H,H}$ = 5.6 Hz, 2H, OC**H**$_2$); due to overlapping resonances, as well in 2D spectra, signals for PC**H**$_2$ could not be localized exactly. ^{13}C{^{1}H} NMR (126 MHz, C_6D_6): δ [ppm] = 5.1

(s, Si(**C**H$_3$)$_3$), 10.5 (s, Ga**C**H), 23.7 (d, $^1J_{P,C}$ = 54.5 Hz, P**C**H$_2$), 25.9 (s, C(**C**H$_3$)$_3$), 26.2 (s, C(**C**H$_3$)$_3$), 33.6 (d, $^1J_{P,C}$ = 58.9 Hz, **C**(CH$_3$)$_3$), 35.4 (d, $^1J_{P,C}$ = 58.3 Hz, **C**(CH$_3$)$_3$), 60.5 (d, $^2J_{P,C}$ = 7.6 Hz, O**C**H$_2$). ^{29}Si{^{1}H} NMR (99 MHz, C$_6$D$_6$): δ [ppm] = –0.5 (s). ^{31}P{^{1}H} NMR (202 MHz, C$_6$D$_6$): δ [ppm] = 75.1 (s).

Bis$_2$Ga–O–P^{t}Bu$_2$·PO (**8**): Using propylene oxide (10 µL, 8.3 mg, 143 µmol, 1.5 equiv.), the ring-opening adduct **8** crystallized from *n*-hexane at –18 °C, giving colourless needles (32 mg, 53 µmol, 55%). ^{1}H NMR (500 MHz, C$_6$D$_6$): δ [ppm] = –0.49 (s, 1H, GaC**H**), –0.39 (s, 1H, GaC**H**), 0.42 – 0.56 (m, 36H, Si(C**H**$_3$)$_3$), 0.85 (d, $^3J_{P,H}$ = 13.9 Hz, 9H, C(C**H**$_3$)$_3$), 0.90 (d, $^3J_{P,H}$ = 14.0 Hz, 9H, C(C**H**$_3$)$_3$), 1.32 (ddd, *J* =14.8, 3.7, 1.8 Hz, PC**H**$_2$), 1.36 (dd, *J* =5.7, 2.7 Hz, C**H**$_3$), 1.63 (ddd, *J* =14.8, 10.8, 8.8 Hz, PC**H**$_2$), 4.35 (m, 1H, OC**H**). ^{13}C{^{1}H} NMR (126 MHz, C$_6$D$_6$): δ [ppm] = 4.8 (s, overlapped, from ^{1}H-^{13}C HSQC experiment, Ga**C**H), 4.9 (s, Si(**C**H$_3$)$_3$), 5.2 (s, Si(**C**H$_3$)$_3$), 5.6 (s, Si(**C**H$_3$)$_3$), 5.6 (s, overlapped, from ^{1}H-^{13}C HSQC experiment, Ga**C**H), 26.2 (s, C(**C**H$_3$)$_3$), 26.5 (s, C(**C**H$_3$)$_3$), 29.4 (d, $^3J_{P,C}$ = 13.6 Hz, **C**H$_3$), 30.0 (d, $^1J_{P,C}$ = 54.5 Hz, P**C**H$_2$), 35.1 (d, $^1J_{P,C}$ = 57.7 Hz, **C**(CH$_3$)$_3$), 35.7 (d, $^1J_{P,C}$ = 59.0 Hz, **C**(CH$_3$)$_3$), 65.6 (d, $^2J_{P,C}$ = 5.9 Hz, O**C**H). ^{29}Si{^{1}H} NMR (99 MHz, C$_6$D$_6$): δ [ppm] = –1.7 (s), –1.1 (s), –0.7 (s), –0.2 (s). ^{31}P{^{1}H} NMR (202 MHz, C$_6$D$_6$): δ [ppm] = 73.0 (s). Elemental analysis calcd (%) for C$_{25}$H$_{62}$GaO$_2$PSi$_4$ (M_r = 607.81): C 49.40, H 10.28; found C 49.14, H 10.53.

Bis$_2$Ga–O–P^{t}Bu$_2$·PhC≡CH (**9**): Using phenylacetylene (10 µL, 9.3 mg, 91 µmol, 1.0 equiv.) and stirring at 70 °C, **9a** was recrystallized from *n*-hexane at –18 °C, giving colourless needles of the deprotonation product (38 mg, 59 µmol, 64%). ^{1}H NMR (500 MHz, C$_6$D$_6$): δ [ppm] = –0.31 (s, 2H, GaC**H**), 0.46 (s, 36H, Si(C**H**$_3$)$_3$), 0.95 (d, $^3J_{P,H}$ = 15.7 Hz, 18H, C(C**H**$_3$)$_3$), 5.98 (d, $^1J_{P,H}$ = 440.1 Hz, 1H, P**H**), 6.98 (t, $^3J_{H,H}$ = 7.4 Hz, 1H, *para*-**H**), 7.05 (t, $^3J_{H,H}$ = 7.3 Hz, 2H, *meta*-**H**), 7.62 (d, $^3J_{H,H}$ = 7.8 Hz, 2H, *ortho*-**H**). ^{13}C{^{1}H} NMR (126 MHz, C$_6$D$_6$): δ [ppm] = 4.6 (s, Si(**C**H$_3$)$_3$), 10.0 (s, Ga**C**H), 26.0 (s, C(**C**H$_3$)$_3$), 33.8 (d, $^1J_{P,C}$ = 58.4 Hz, **C**(CH$_3$)$_3$), 109.7 (s, PhC≡**C**Ga), 126.1 (s, Ph**C**≡CGa), 127.6 (s, *para*-**C**), 128.4 (s, *ipso*-**C**), 128.6 (s, *meta*-**C**), 131.6 (s, *ortho*-**C**). ^{29}Si{^{1}H} NMR (99 MHz, C$_6$D$_6$): δ [ppm] = –0.9 (s). ^{31}P{^{1}H} NMR (202 MHz, C$_6$D$_6$): δ [ppm] = 67.3 (s). Elemental analysis calcd (%) for C$_{30}$H$_{62}$GaOPSi$_4$ (M_r = 651.86): C 55.28, H 9.59; found C 54.61, H 9.88.

Bis$_2$Ga–O–P^{t}Bu$_2$·Me$_3$SiC≡CH (**10**): Using trimethylsilylacetylene (10 µL, 7.1 mg, 72 µmol, 1.0 equiv.), stirring at 70 °C and after an additional washing step with *n*-hexane, **10** was obtained in a colourless resin-like form (41 mg, 63 µmol, 92%). *Deprotonation product* (**10a**): ^{1}H NMR (500 MHz, C$_6$D$_6$): δ [ppm] = –0.50 (s, 2H, GaC**H**), 0.27 (s, 9H, Si(C**H**$_3$)$_3$), 0.46 (s, 36H, CH(Si(C**H**$_3$)$_3$)$_2$), 0.96 (d, $^3J_{P,H}$ = 15.6 Hz, 18H, C(C**H**$_3$)$_3$), 5.97 (d, $^1J_{P,H}$ = 442.2 Hz, 1H, P**H**). ^{13}C{^{1}H} NMR (126 MHz, C$_6$D$_6$): δ [ppm] = 0.3 (s, Si(**C**H$_3$)$_3$), 4.8 (s, Si(**C**H$_3$)$_3$), 8.2 (s, Ga**C**H), 26.2 (s, C(**C**H$_3$)$_3$), 33.8 (d, $^1J_{P,C}$ = 58.3 Hz, **C**(CH$_3$)$_3$), 115.7 (s, Me$_3$SiC≡**C**Ga), 134.8 (s, Me$_3$Si**C**≡CGa). ^{29}Si{^{1}H} NMR (99 MHz, C$_6$D$_6$): δ [ppm] = –22.9 (s), –0.7 (s). ^{31}P{^{1}H} NMR (202 MHz, C$_6$D$_6$): δ [ppm] = 66.9 (s). Elemental analysis calcd (%) for C$_{27}$H$_{66}$GaOPSi$_5$ (M_r = 647.95): C 50.05, H 10.27; found C 49.81, H 10.37. *Ring-closure product* (**10b**): ^{1}H NMR (500 MHz, C$_6$D$_6$): δ [ppm] = –0.50 (br. s, 2H, GaC**H**), 0.18 (s, 9H, Si(C**H**$_3$)$_3$), 0.38 – 0.43 (s, 36H, CH(Si(C**H**$_3$)$_3$)$_2$), 1.02 (d, $^3J_{P,H}$ = 14.0 Hz, 18H, C(C**H**$_3$)$_3$), 9.25 (d, $^3J_{P,H}$ = 56.0 Hz, 1H, PC**H**). ^{13}C{^{1}H} NMR (126 MHz, C$_6$D$_6$): δ [ppm] = 2.0 (s, Si(**C**H$_3$)$_3$), 5.1/5.4 (s, Si(**C**H$_3$)$_3$), 27.5 (s, C(**C**H$_3$)$_3$), 35.1 (d, $^1J_{P,C}$ = 56.3 Hz, **C**(CH$_3$)$_3$), 139.9 (d, $^1J_{P,C}$ = 41.4 Hz, GaC=**C**P), 206.7 (d, $^2J_{P,C}$ = 5.9

Hz, Ga**C**=CP); a signal for Ga**C**H could not be observed. $^{29}Si\{^1H\}$ NMR (99 MHz, C_6D_6): δ [ppm] = −8.2 (s), −1.6 (s). $^{31}P\{^1H\}$ NMR (202 MHz, C_6D_6): δ [ppm] = 84.8 (s).

Bis$_2$(Cl)Ga–O–P(Bn)^{t}Bu$_2$ (**11**): Using benzyl chloride (10 µL, 9.1 mg, 72 µmol, 1.0 equiv.), stirring at 70 °C and after an additional washing step with *n*-hexane, **11** was obtained as a light yellow solid (44 mg, 65 µmol, 94%). ^1H NMR (500 MHz, C_6D_6): δ [ppm] = −0.06 (s, 2H, GaC**H**), 0.36 (s, 36H, Si(C**H**$_3$)$_3$), 1.06 (d, $^3J_{P,H}$ = 13.6 Hz, 18H, C(C**H**$_3$)$_3$), 3.40 (d, $^3J_{P,H}$ = 14.0 Hz, 2H, C**H**$_2$), 7.00 (t, $^3J_{H,H}$ = 7.3 Hz, 1H, *para*-**H**), 7.05 (t, $^3J_{H,H}$ = 7.6 Hz, 2H, *meta*-**H**), 7.39 (d, $^3J_{H,H}$ = 7.9 Hz, 2H, *ortho*-**H**). $^{13}C\{^1H\}$ NMR (126 MHz, C_6D_6): δ [ppm] = 4.3 (s, Si(**C**H$_3$)$_3$), 15.8 (s, Ga**C**H), 27.5 (s, C(**C**H$_3$)$_3$), 31.2 (d, $^1J_{P,C}$ = 48.4 Hz, **C**H$_2$), 36.7 (d, $^1J_{P,C}$ = 56.3 Hz, **C**(CH$_3$)$_3$), 127.0 (d, $^4J_{P,C}$ = 2.5 Hz, *para*-**C**), 128.7 (s, *meta*-**C**), 130.8 (d, $^3J_{P,C}$ = 5.0 Hz, *ortho*-**C**), 134.3 (d, $^2J_{P,C}$ = 6.0 Hz, *ipso*-**C**). $^{29}Si\{^1H\}$ NMR (99 MHz, C_6D_6): δ [ppm] = −1.3 (s). $^{31}P\{^1H\}$ NMR (202 MHz, C_6D_6): δ [ppm] = 63.6 (s). Elemental analysis calcd (%) for $C_{29}H_{63}GaOPSi_4$ (M_r = 676.31): C 51.50, H 9.39; found C 51.67, H 9.59.

2) NMR spectra

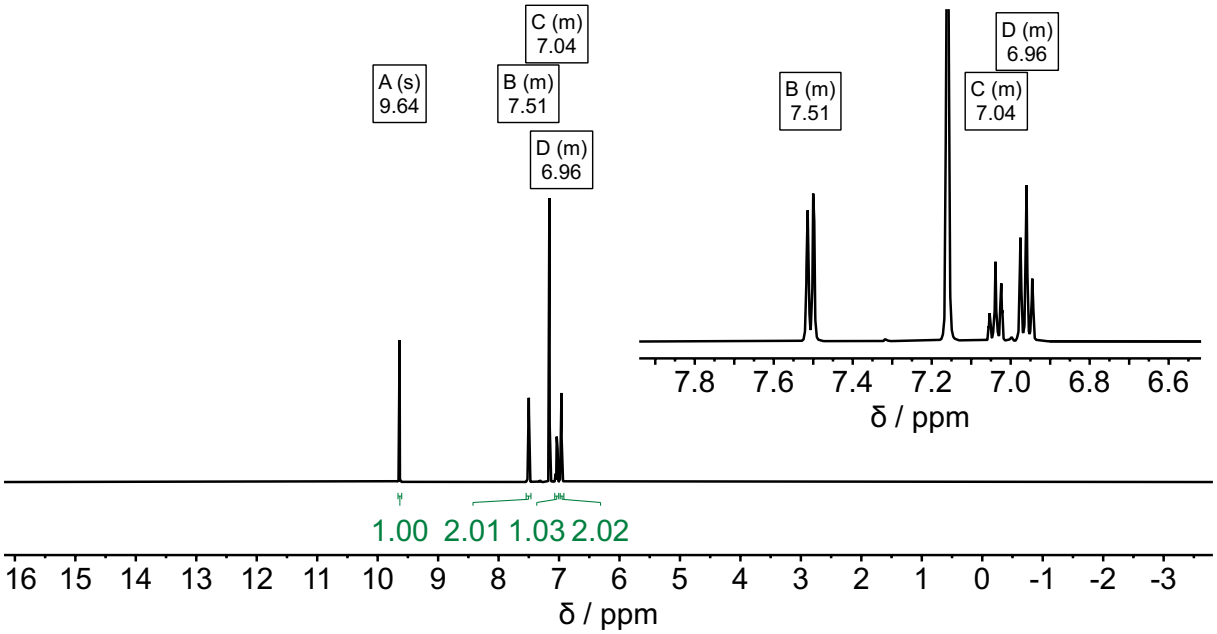

Figure S1. ^{1}H NMR spectrum of benzaldehyde (PhCHO) in C_6D_6 (500 MHz, 298K).

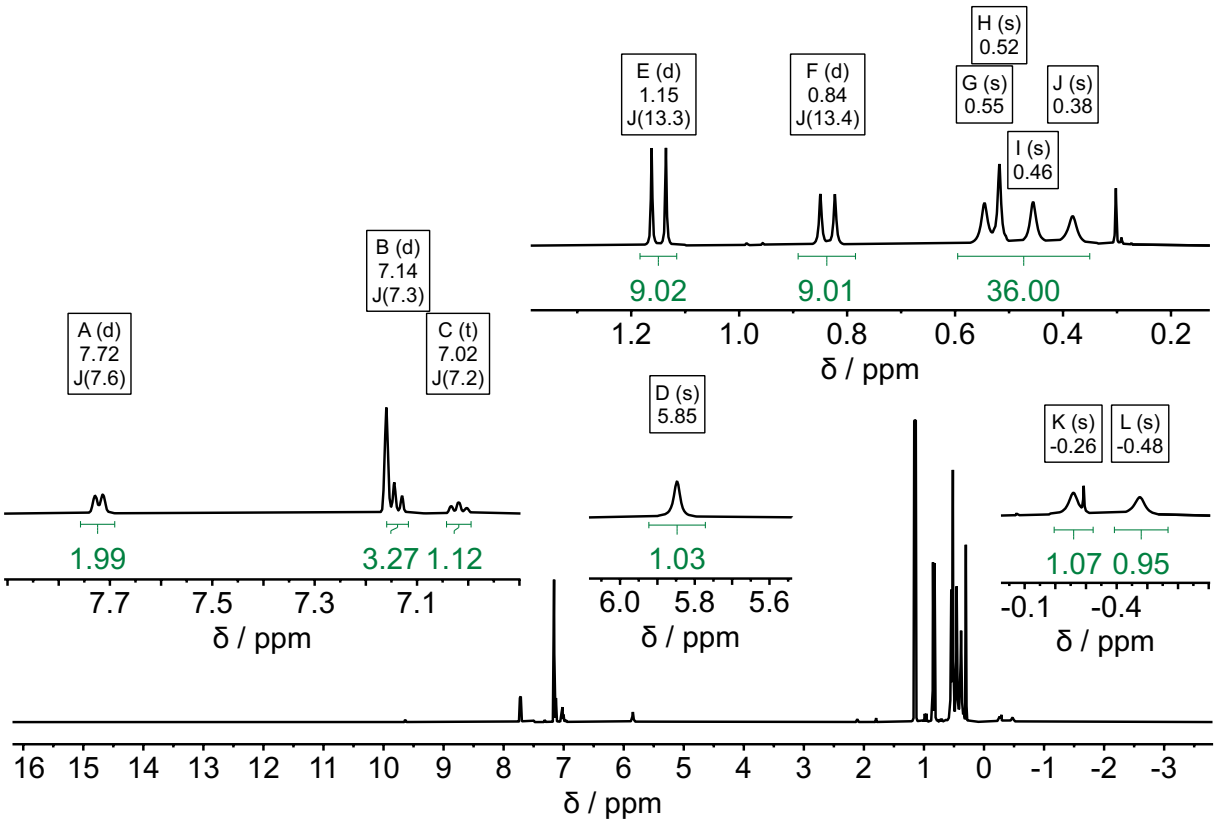

Figure S2. ^{1}H NMR spectrum of $Bis_2Ga–O–P^tBu_2$·PhCHO (**1**) in C_6D_6 (500 MHz, 298K): δ [ppm] = –0.48 (s, 1H, GaC**H**), –0.26 (s, 1H, GaC**H**), 0.36 – 0.58 (m, 36H, Si(C**H**$_3$)$_3$), 0.84 (d, $^{3}J_{P,H}$ = 13.4 Hz, 9H, C(C**H**$_3$)$_3$), 1.15 (d, $^{3}J_{P,H}$ = 13.3 Hz, 9H, C(C**H**$_3$)$_3$), 5.85 (s, C**H**O), 7.02 (t, $^{3}J_{H,H}$ = 7.2 Hz, 1H, *para*-**H**), 7.14 (t, $^{3}J_{H,H}$ = 7.3 Hz, 2H, *meta*-**H**), 7.72 (d, $^{3}J_{H,H}$ = 7.6 Hz, 2H, *ortho*-**H**).

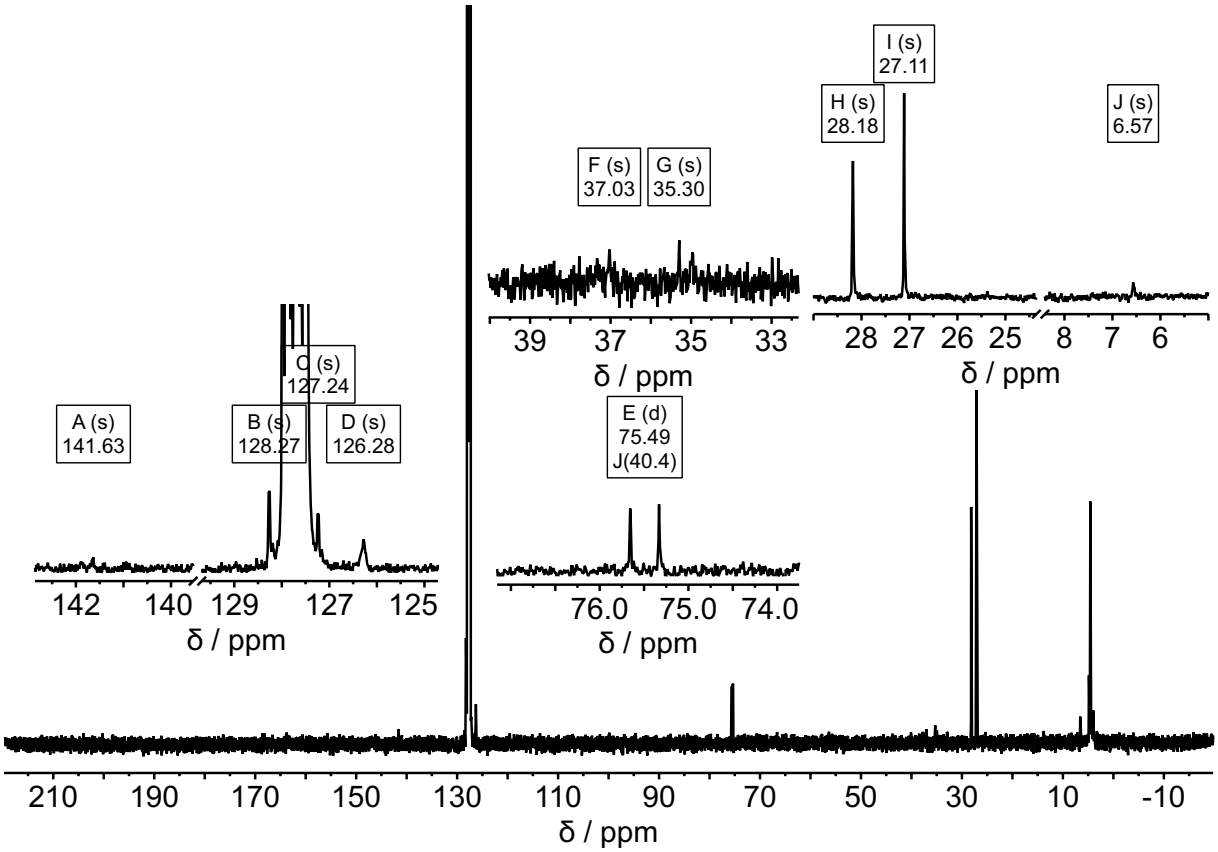

Figure S3. $^{13}C\{^{1}H\}$ NMR spectrum of $Bis_2Ga–O–P^tBu_2$·PhCHO (**1**) in C_6D_6 (126 MHz, 298K): δ [ppm] = 3.9 (s, Si(**C**H_3)$_3$), 4.6(s, Si(**C**H_3)$_3$), 4.6 (s, Si(**C**H_3)$_3$), 4.8 (s, Si(**C**H_3)$_3$), 6.6 (s, Ga**C**H), 27.1 (s, C(**C**H_3)$_3$), 28.2 (s, C(**C**H_3)$_3$), 35.3 (s, **C**$(CH_3)_3$), 37.0 (s, **C**$(CH_3)_3$), 75.5 (d, $^{1}J_{P,C}$ = 40.4 Hz, **C**HO), 126.3 (s, *ortho*-**C**), 127.2 (s, *para*-**C**), 128.3 (s, *meta*-**C**), 141.6 (s, *ipso*-**C**).

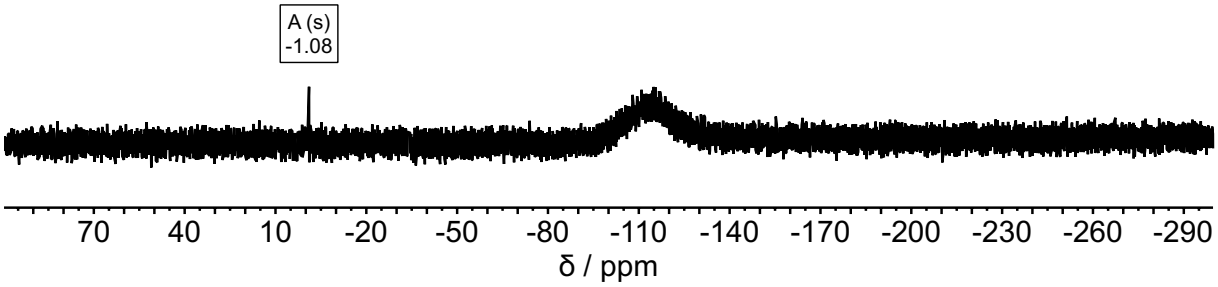

Figure S4. $^{29}Si\{^{1}H\}$ NMR spectrum of $Bis_2Ga–O–P^tBu_2$·PhCHO (**1**) in C_6D_6 (99 MHz, 298K).

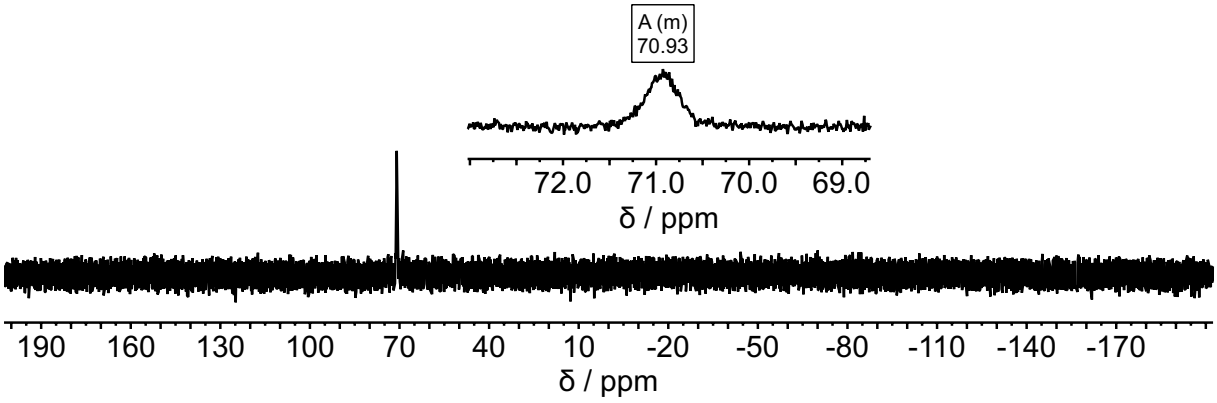

Figure S5. ^{31}P NMR spectrum of $Bis_2Ga–O–P^tBu_2$·PhCHO (**1**) in C_6D_6 (202 MHz, 298K).

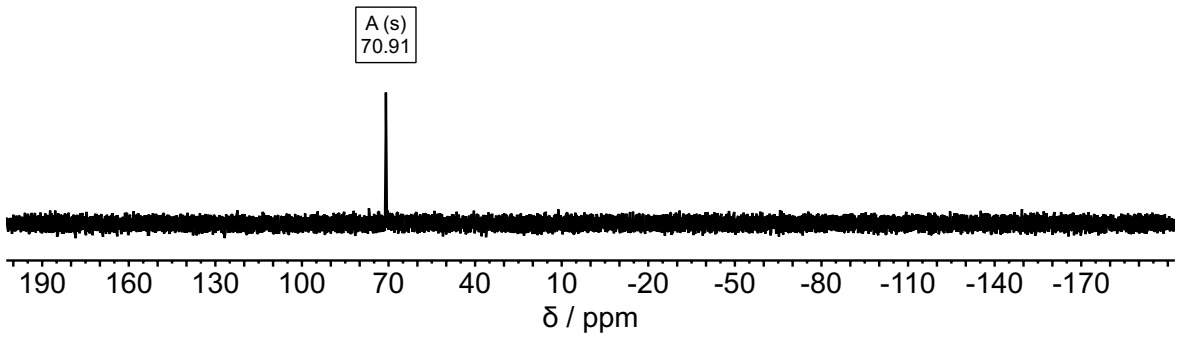

Figure S6. $^{31}P\{^{1}H\}$ NMR spectrum of $Bis_2Ga–O–P^tBu_2$·PhCHO (**1**) in C_6D_6 (202 MHz, 298K).

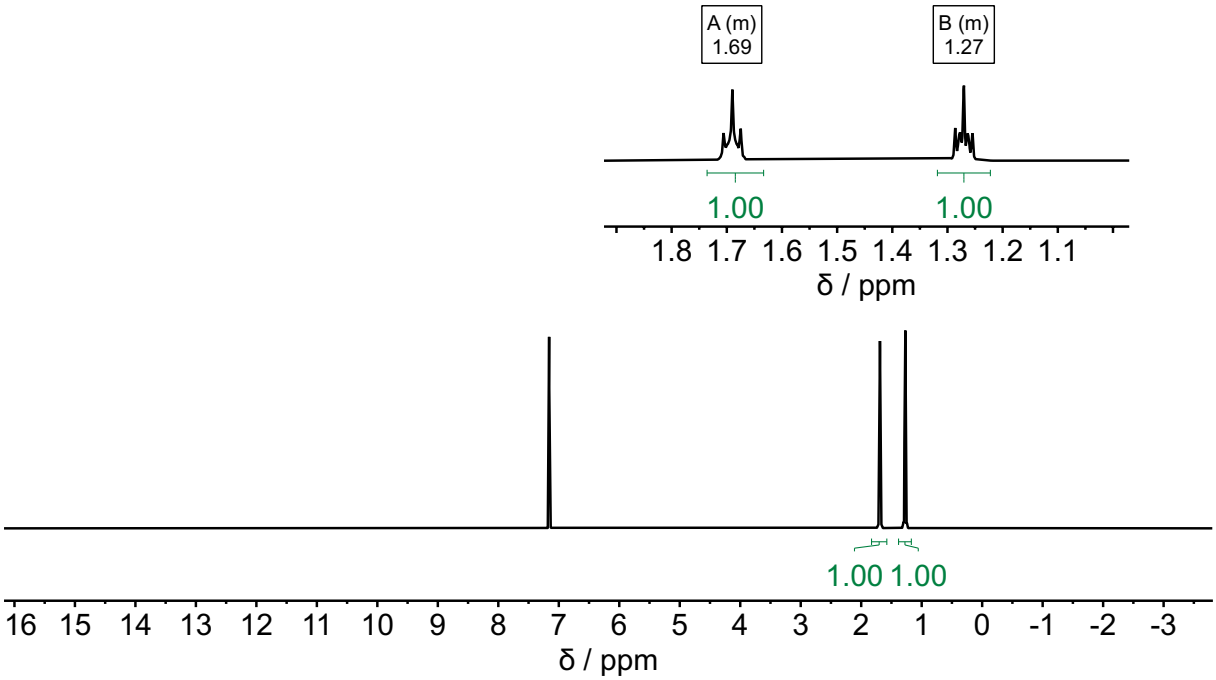

Figure S7. ^{1}H NMR spectrum of cyclopentanone (CP) in C_6D_6 (500 MHz, 298K).

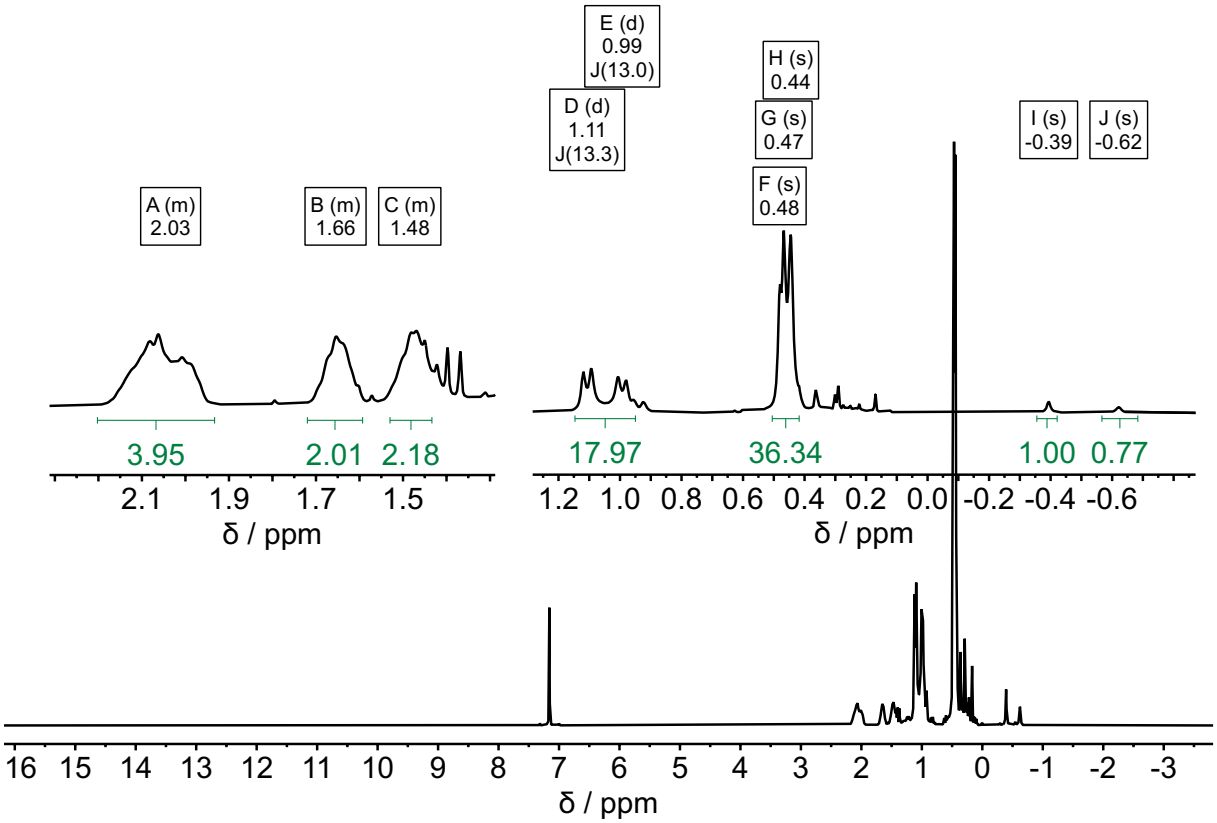

Figure S8. ^{1}H NMR spectrum of Bis$_2$Ga–O–P^{t}Bu$_2$·CP (**2**) in C_6D_6 (500 MHz, 298K): δ [ppm] = –0.62 (s, 1H, GaC**H**), –0.39 (s, 1H, GaC**H**), 0.42 – 0.50 (s, 36H, Si(C**H**$_3$)$_3$), 0.99 (d, $^{3}J_{P,H}$ = 13.0 Hz, 9H, C(C**H**$_3$)$_3$), 1.11 (d, $^{3}J_{P,H}$ = 13.3 Hz, 9H, C(C**H**$_3$)$_3$), 1.48(m, 2H, C**H**$_2$), 1.66 (m, 2H, C**H**$_2$), 2.03 (m, 4H, C**H**$_2$).

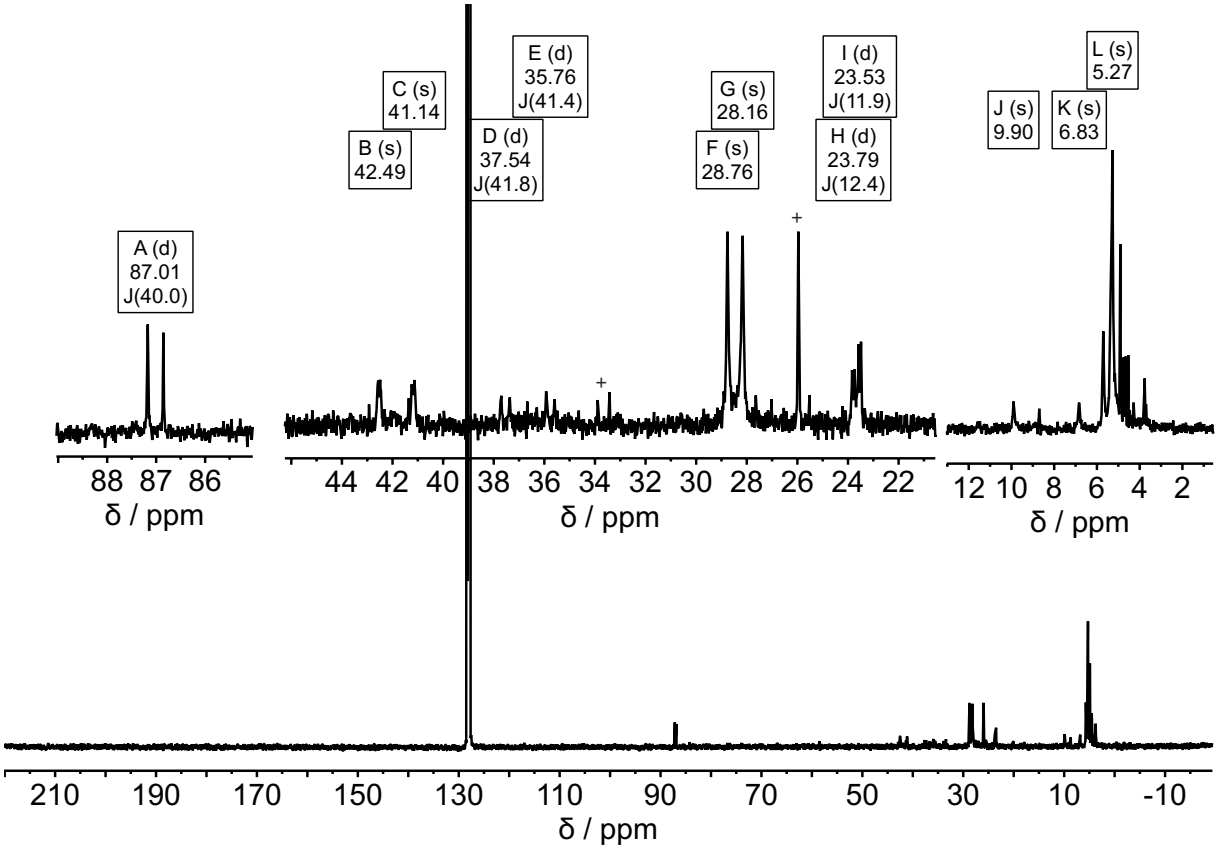

Figure S9. ^{13}C{^{1}H} NMR spectrum of Bis$_2$Ga–O–P^{t}Bu$_2$·CP (**2**) in C_6D_6 (126 MHz, 298K): δ [ppm] = 5.3 (s, Si(**C**H$_3$)$_3$), 6.8 (s, Ga**C**H), 9.9 (s, Ga**C**H), 23.5 (d, $^{2}J_{P,C}$ = 11.9 Hz, **C**H$_2$), 23.8 (d, $^{2}J_{P,C}$ = 12.4 Hz, **C**H$_2$), 28.2 (s,

C(**C**H$_3$)$_3$), 28.8 (s, C(**C**H$_3$)$_3$), 35.8 (d, $^1J_{P,C}$ = 41.4 Hz, **C**(CH$_3$)$_3$), 37.5 (d, $^1J_{P,C}$ = 41.8 Hz, **C**(CH$_3$)$_3$), 41.1 (s, **C**H$_2$), 42.5 (s, **C**H$_2$), 87.0 (d, $^1J_{P,C}$ = 40.0 Hz, P**C**O). Signals resulting from partial hydrolysis (^{t}Bu$_2$P(O)H) are denoted with +.

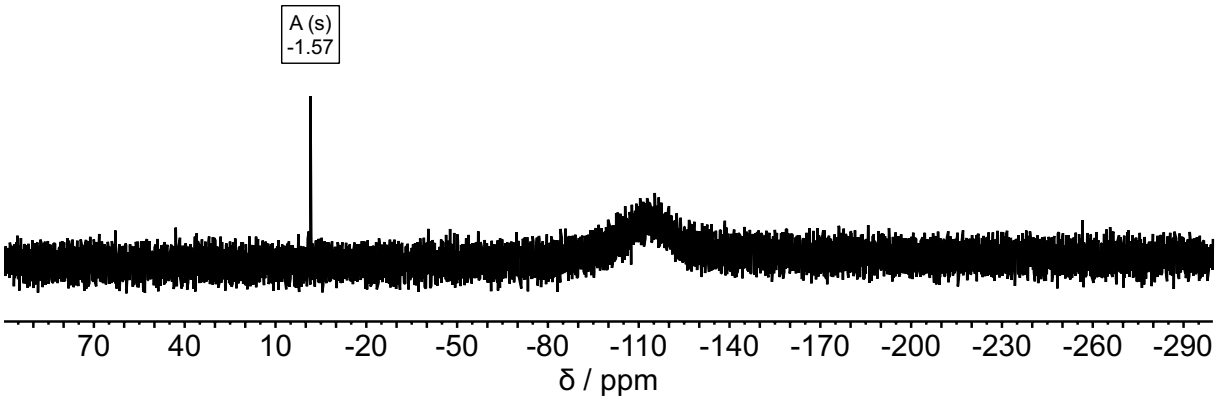

Figure S10. ^{29}Si{^{1}H} NMR spectrum of Bis$_2$Ga–O–P^{t}Bu$_2$·CP (**2**) in C$_6$D$_6$ (99 MHz, 298K).

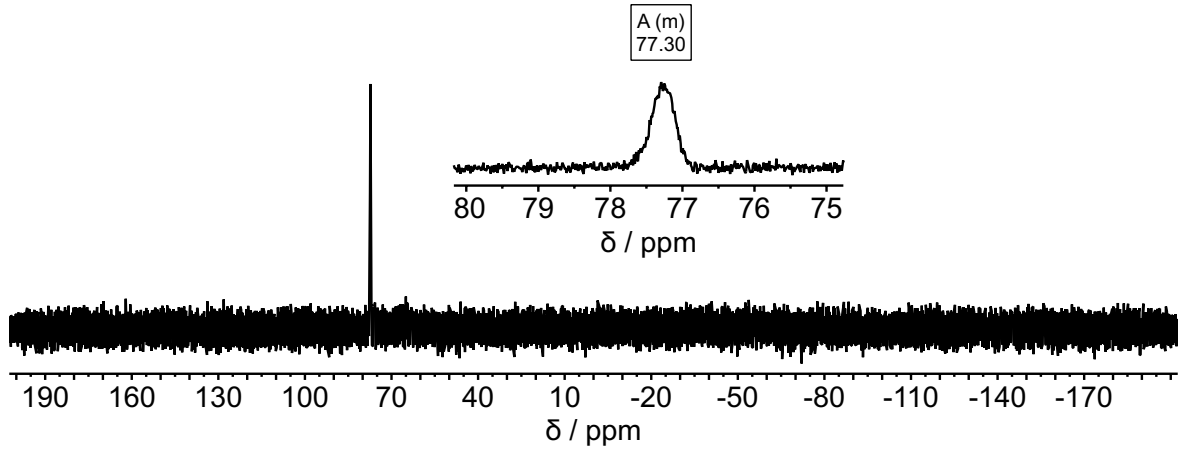

Figure S11. ^{31}P NMR spectrum of Bis$_2$Ga–O–P^{t}Bu$_2$·CP (**2**) in C$_6$D$_6$ (202 MHz, 298K).

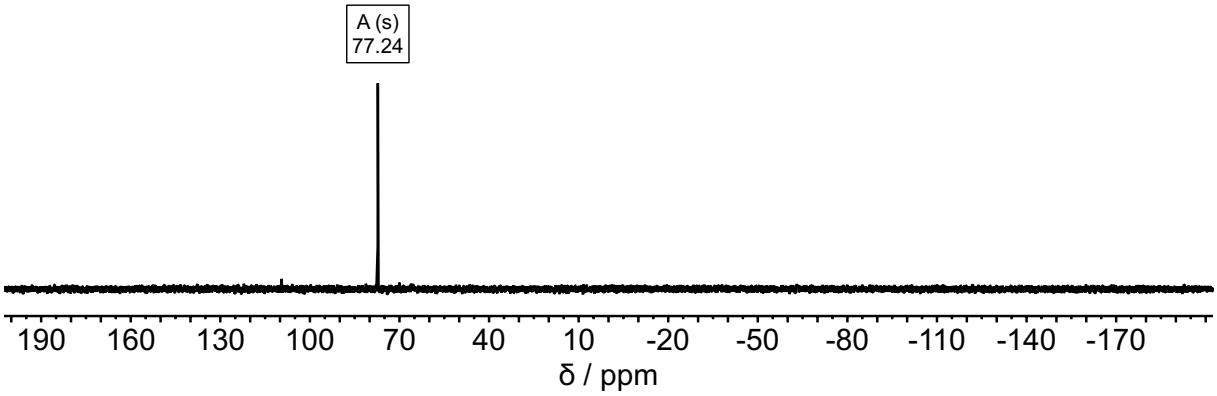

Figure S12. ^{31}P{^{1}H} NMR spectrum of Bis$_2$Ga–O–P^{t}Bu$_2$·CP (**2**) in C$_6$D$_6$ (202 MHz, 298K).

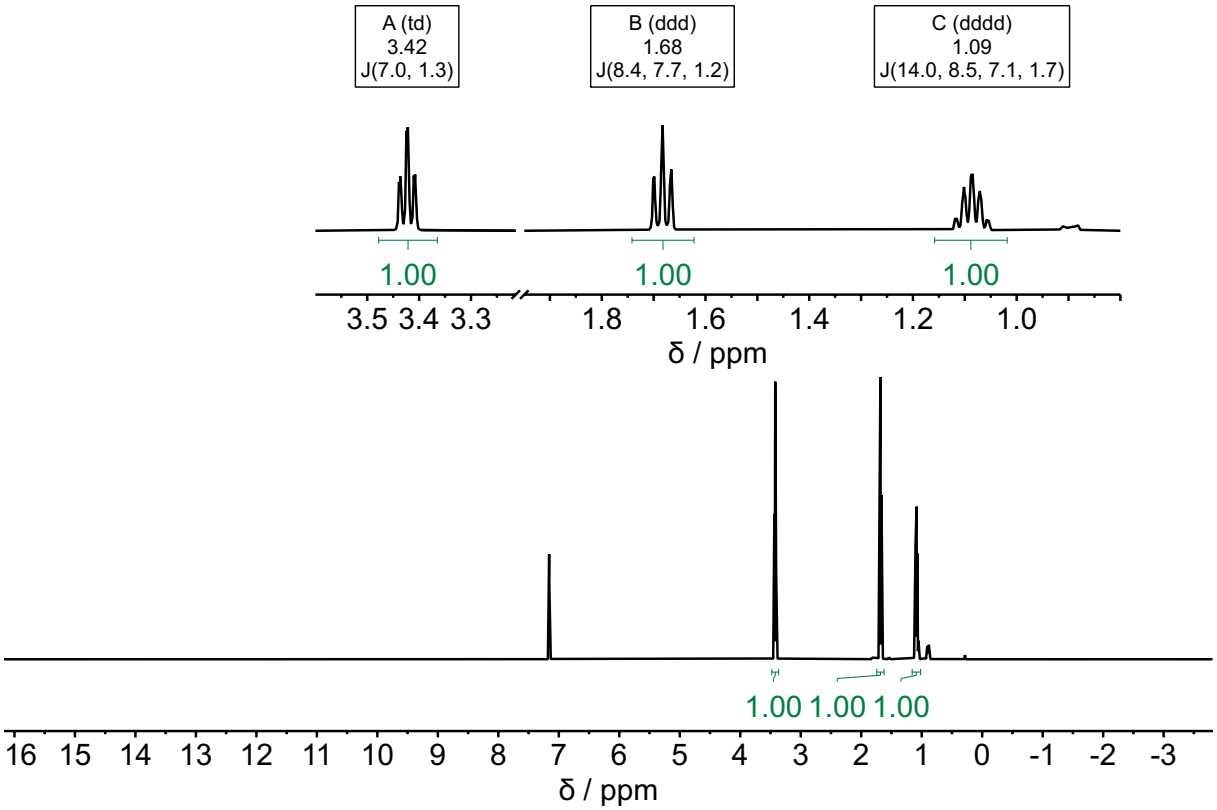

Figure S13. ^{1}H NMR spectrum of *γ*-butyrolactone (GBL) in C_6D_6 (500 MHz, 298K).

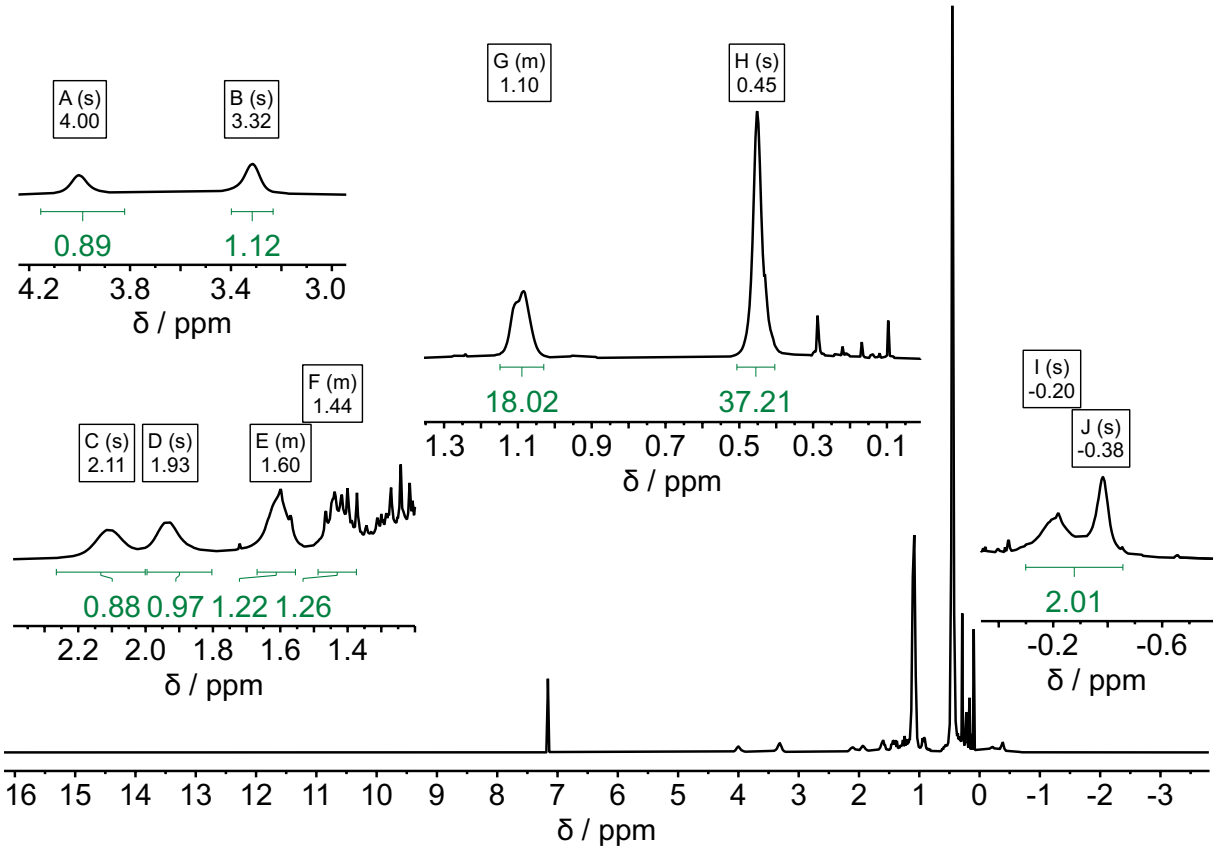

Figure S14. ^{1}H NMR spectrum of $Bis_2Ga–O–P^tBu_2$·GBL (**3**) in C_6D_6 (500 MHz, 298K): *δ* [ppm] = –0.38 (br. s, 1H, GaC**H**), –0.20 (br. s, 1H, GaC**H**), 0.45 (s, 36H, $Si(CH_3)_3$), 1.10 (m, 18H, $C(CH_3)_3$), 1.44 (m, 1H, CH_2), 1.60 (br. m, 1H, CH_2), 1.93 (br. s, 1H, CH_2), 2.11 (br. s, 1H, CH_2), 3.32 (br. s, 1H, CH_2), 4.00 (br. s, 1H, CH_2).

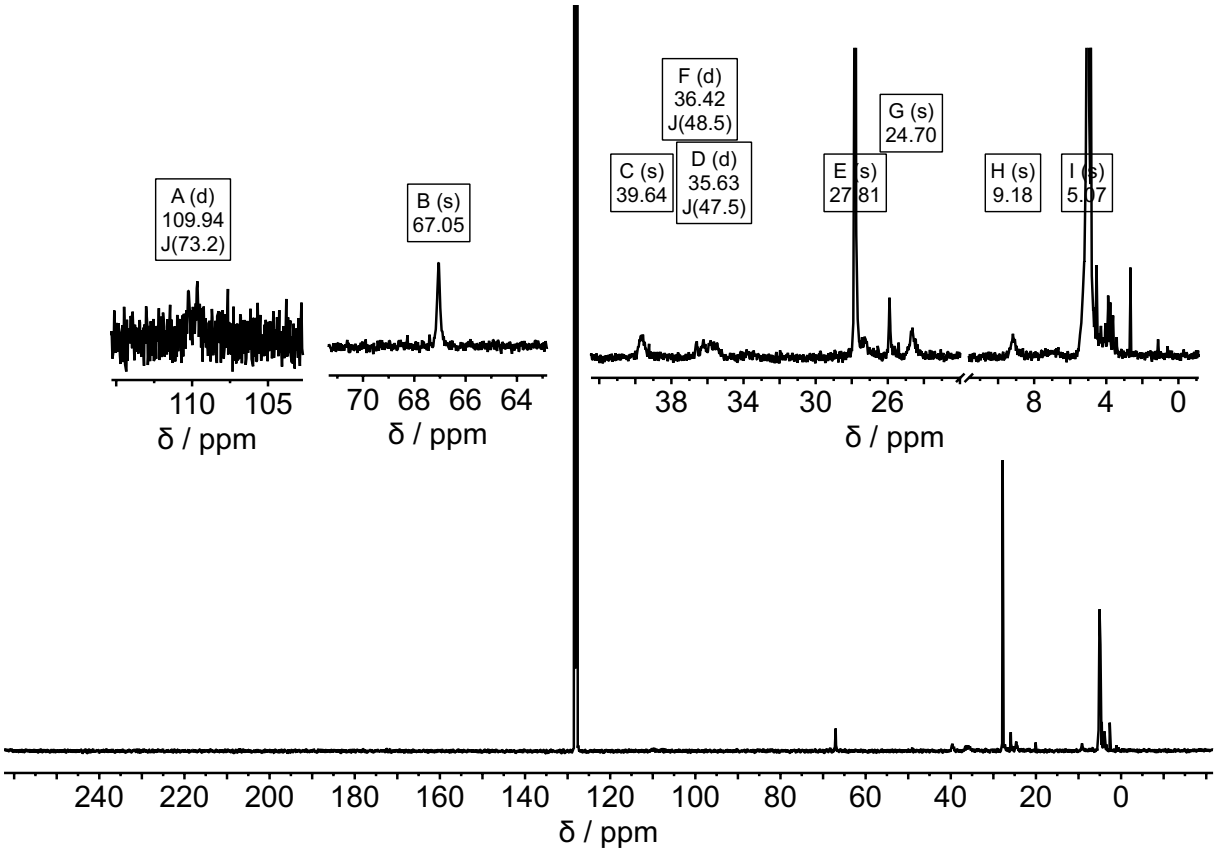

Figure S15. $^{13}C\{^{1}H\}$ NMR spectrum of $Bis_2Ga–O–P^tBu_2$·GBL (**3**) in C_6D_6 (126 MHz, 298K): δ [ppm] = 5.1 (s, $Si(\mathbf{C}H_3)_3$), 9.2 (s, Ga**C**H), 24.7 (s, $\mathbf{C}H_2$), 27.8 (s, $C(\mathbf{C}H_3)_3$), 35.6 (d, $^{1}J_{P,C}$ = 47.5 Hz, $\mathbf{C}(CH_3)_3$), 36.4 (d, $^{1}J_{P,C}$ = 48.5 Hz, $\mathbf{C}(CH_3)_3$), 39.6 (s, $\mathbf{C}H_2$), 67.1 (s, $O\mathbf{C}H_2$), 109.9 (d, $^{1}J_{P,C}$ = 73.2 Hz, $P\mathbf{C}O_2$).

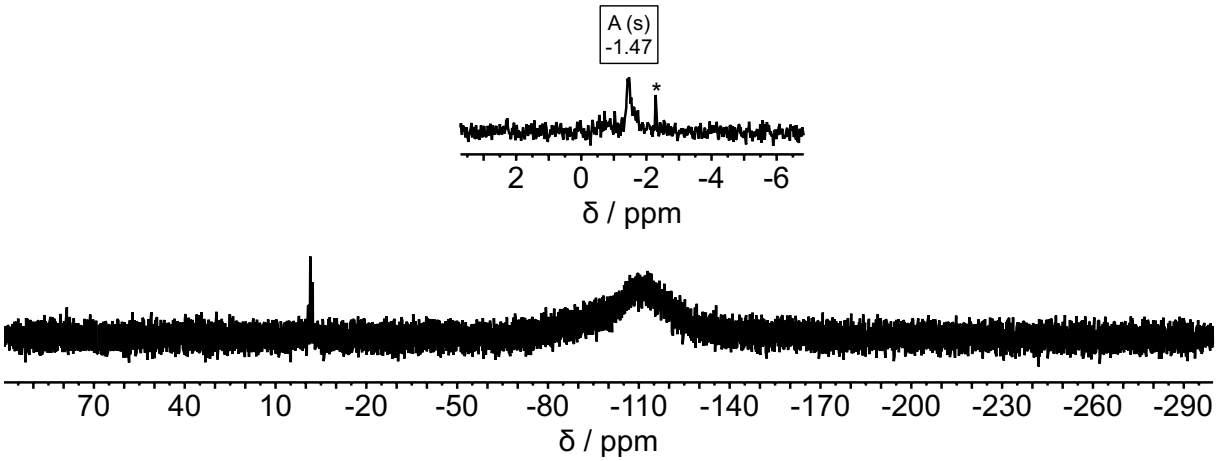

Figure S3. $^{29}Si\{^{1}H\}$ NMR spectrum of $Bis_2Ga–O–P^tBu_2$·GBL (**3**) in C_6D_6 (99 MHz, 298K). The signal denoted with * results from partial hydrolysis (Bis_2GaOH).

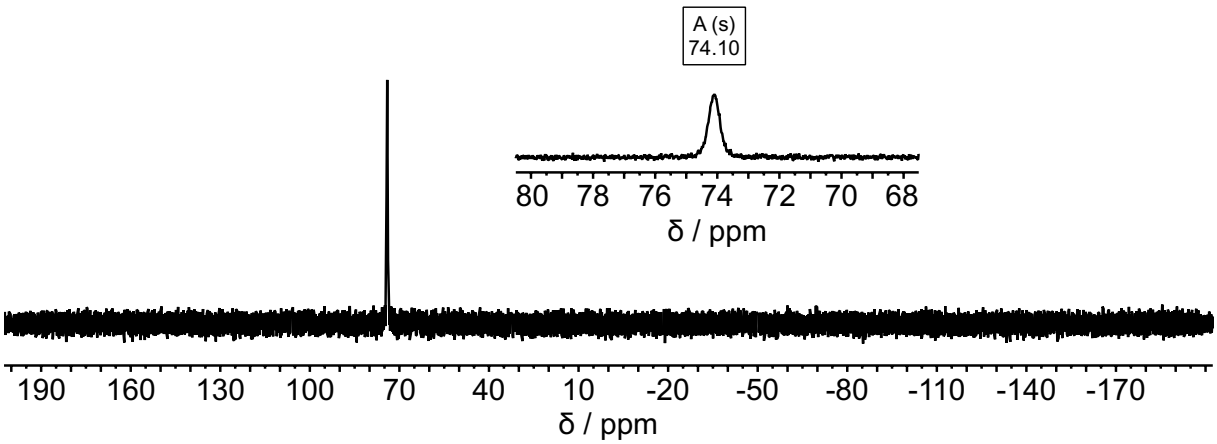

Figure S16. ^{31}P NMR spectrum of Bis$_2$Ga–O–P^{t}Bu$_2$·GBL (**3**) in C_6D_6 (202 MHz, 298K).

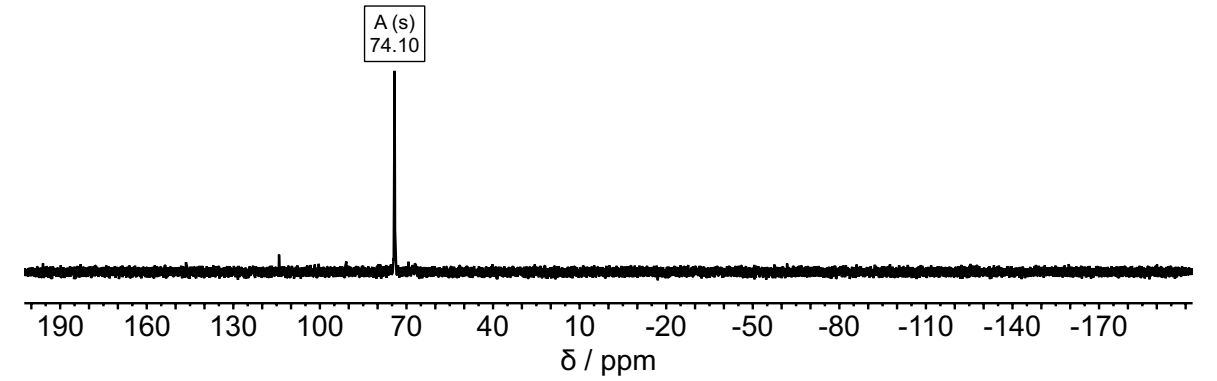

Figure S17. ^{31}P{^{1}H} NMR spectrum of Bis$_2$Ga–O–P^{t}Bu$_2$·GBL (**3**) in C_6D_6 (202 MHz, 298K).

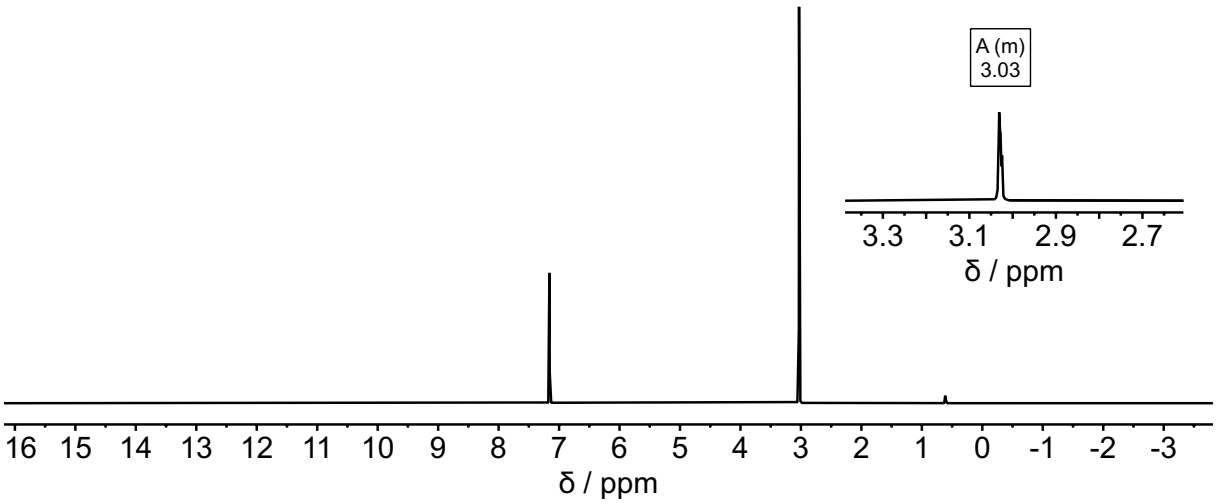

Figure S18. ^{1}H NMR spectrum of ethylene carbonate (EC) in C_6D_6 (500 MHz, 298K).

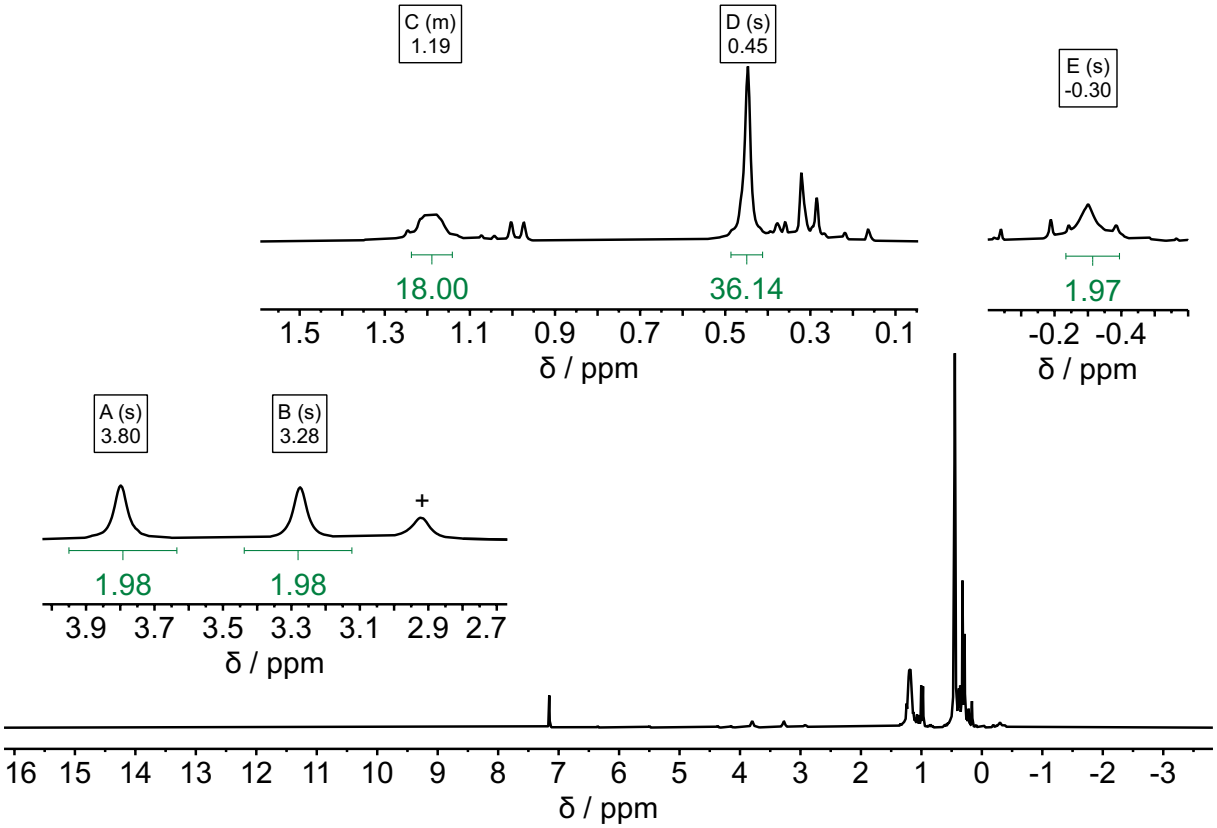

Figure S19. ^{1}H NMR spectrum of $Bis_2Ga–O–P^tBu_2·EC$ (**4**) in C_6D_6 (500 MHz, 298K): δ [ppm] = –0.30 (br. s, 2H, GaC**H**), 0.45 (s, 36H, Si(C**H**$_3$)$_3$), 1.19 (m, 18H, C(C**H**$_3$)$_3$), 3.28 (br. s, 2H, C**H**$_2$), 3.80 (br. s, 2H, C**H**$_2$).

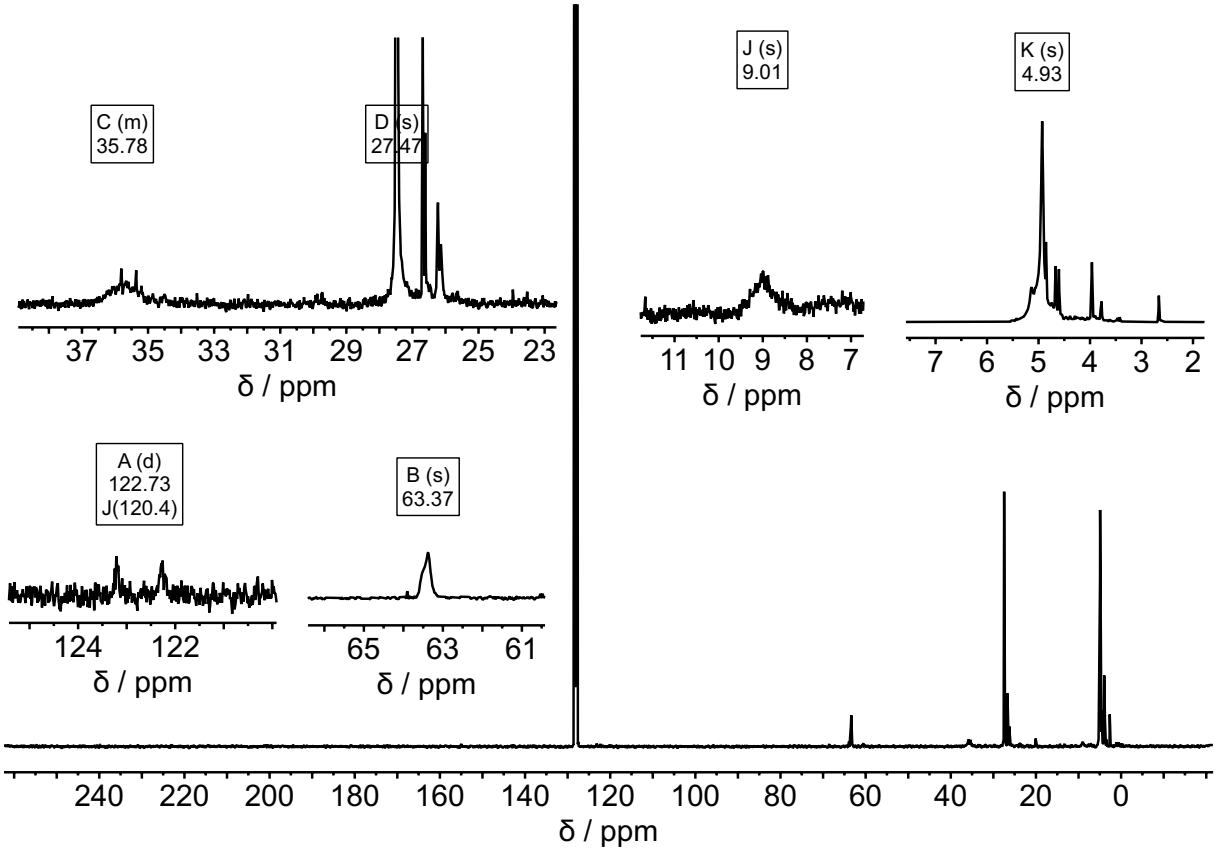

Figure S20. $^{13}C\{^{1}H\}$ NMR spectrum of $Bis_2Ga–O–P^tBu_2·EC$ (**4**) in C_6D_6 (126 MHz, 298K): δ [ppm] = 4.9 (s, Si(**C**H$_3$)$_3$), 9.0 (s, Ga**C**H), 27.5 (s, C(**C**H$_3$)$_3$), 35.8 (br. m, **C**(CH$_3$)$_3$), 63.4 (s, O**C**H$_2$), 122.7 (d, $^{1}J_{P,C}$ = 120.4 Hz, P**C**O$_3$).

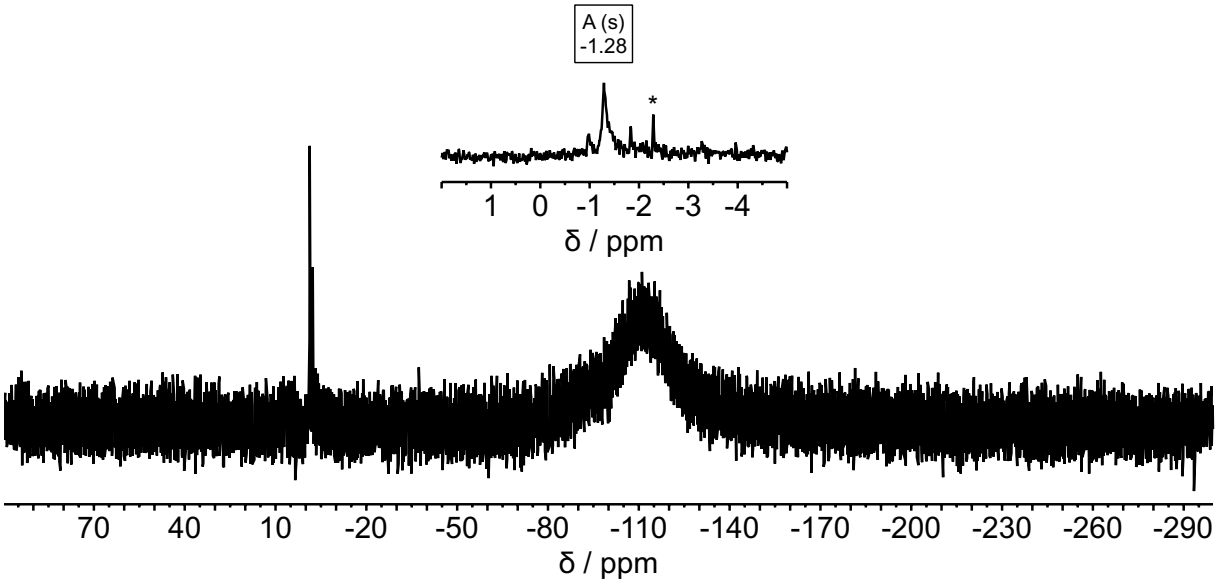

Figure S21. $^{29}Si\{^{1}H\}$ NMR spectrum of $Bis_2Ga–O–P^tBu_2·EC$ (**4**) in C_6D_6 (99 MHz, 298K). The signal denoted with * results from partial hydrolysis (Bis_2GaOH).

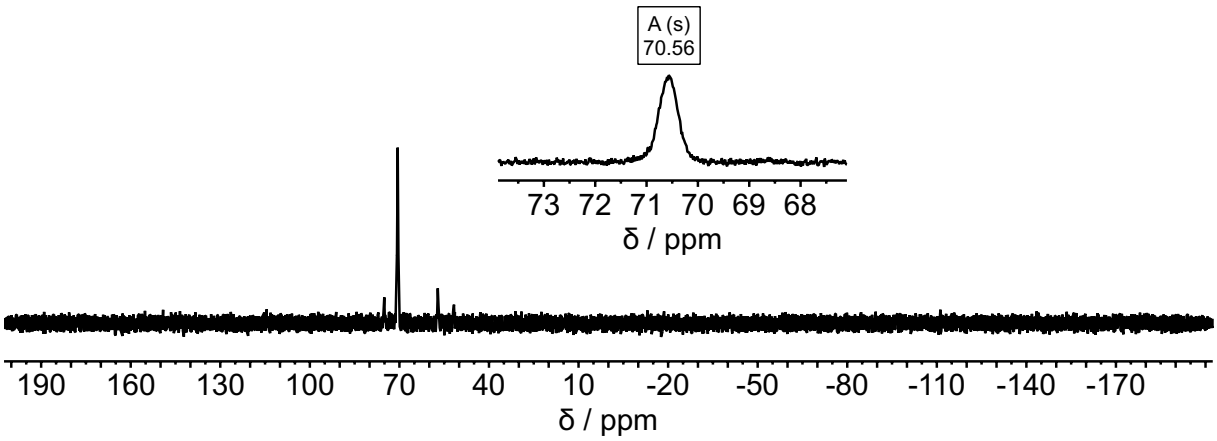

Figure S22. ^{31}P NMR spectrum of $Bis_2Ga–O–P^tBu_2·EC$ (**4**) in C_6D_6 (202 MHz, 298K).

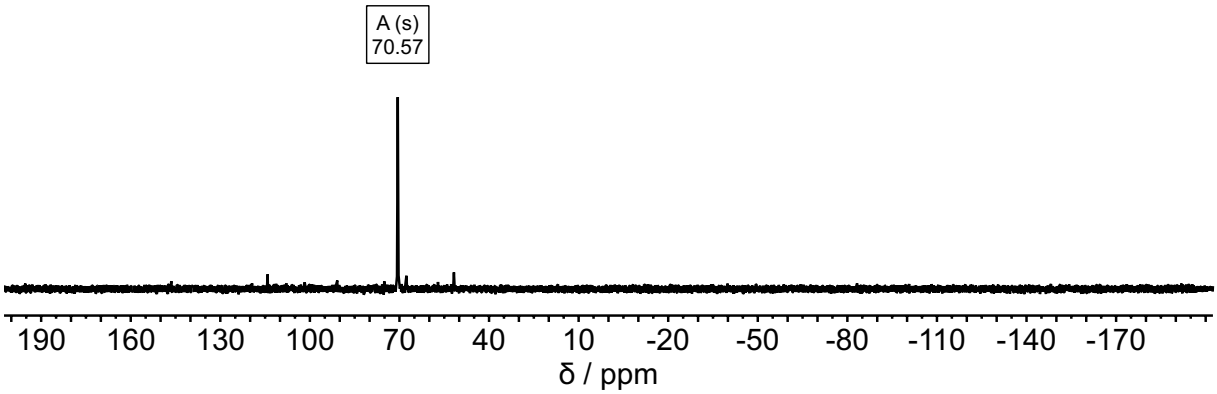

Figure S23. $^{31}P\{^{1}H\}$ NMR spectrum of $Bis_2Ga–O–P^tBu_2·EC$ (**4**) in C_6D_6 (202 MHz, 298K).

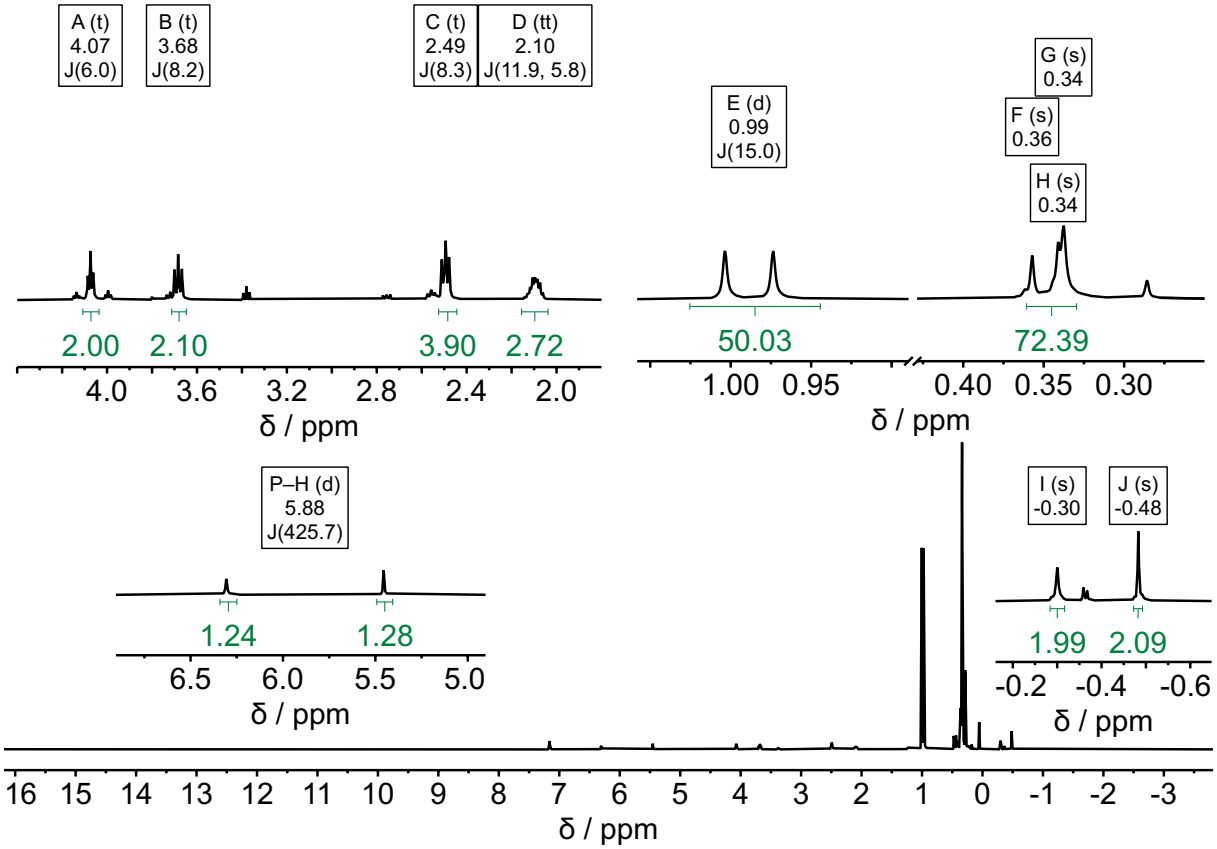

Figure S24. ^{1}H NMR spectrum of **5** in C_6D_6 (500 MHz, 298K): *δ* [ppm] = –0.48 (s, 2H, GaC**H**), –0.30 (s, 2H, GaC**H**), 0.34 (s, 36H, Si(C**H**$_3$)$_3$), 0.34 (s, 18H, Si(C**H**$_3$)$_3$), 0.36 (s, 18H, Si(C**H**$_3$)$_3$), 0.99 (d, $^{3}J_{P,H}$ = 15.0 Hz, 18H, C(C**H**$_3$)$_3$), 2.10 (tt, *J* = 11.9, 5.8 Hz, 2H, C**H**), 2.49 (m, 2H, C**H**), 2.49 (t, *J* = 8.3 Hz, 2H, C**H**), 3.68 (t, *J* = 8.2 Hz, 2H, C**H**), 4.07 (t, *J* = 6.0 Hz, 2H, C**H**$_2$).

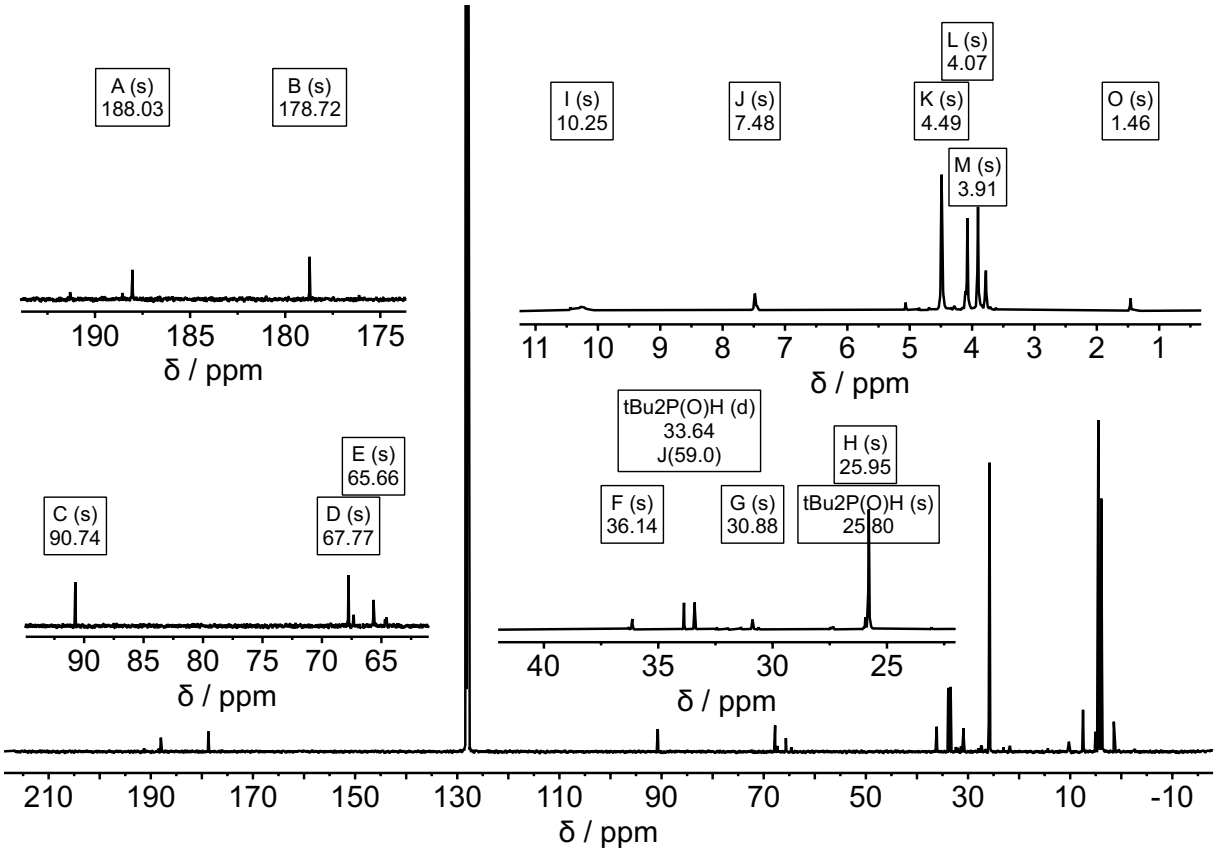

Figure S25. $^{13}C\{^{1}H\}$ NMR spectrum of **5** in C_6D_6 (126 MHz, 298K): δ [ppm] = 3.9/4.1/4.5 (s, Si(**C**H_3)$_3$), 7.5/10.3 (s, Ga**C**H), 25.8 (s, C(**C**H_3)$_3$), 26.0 (s, **C**H_2), 30.9 (s, **C**H_2), 33.6 (d, $^{1}J_{P,C}$ = 59.0 Hz, **C**$(CH_3)_3$), 36.1 (s, **C**H_2), 65.7 (s, O**C**H_2), 67.8 (s, O**C**H_2), 90.7 (s, **C**CO_2Ga), 178.7 (s, **C**O_2Ga), 188.0 (s, **C**=O).

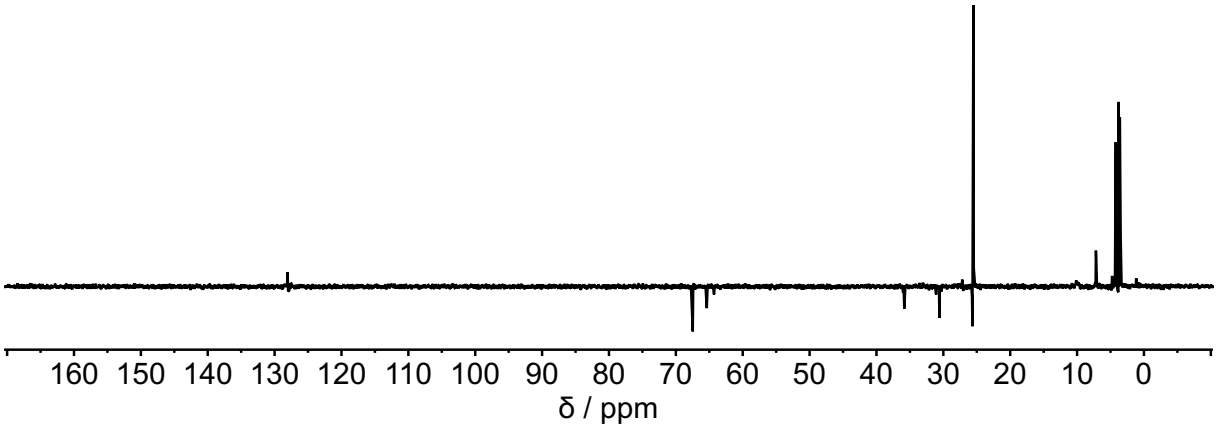

Figure S26. ^{13}C DEPT-135 NMR spectrum of **5** in C_6D_6 (126 MHz, 298K).

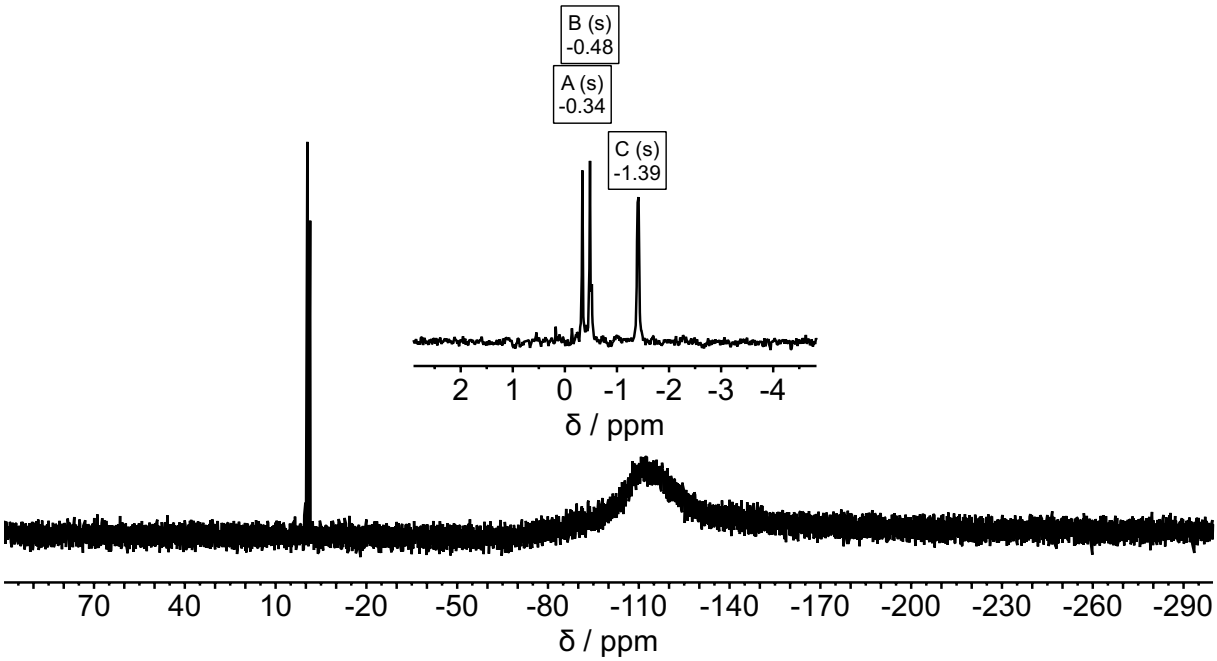

Figure S27. $^{29}Si\{^{1}H\}$ NMR spectrum of **5** in C_6D_6 (99 MHz, 298K).

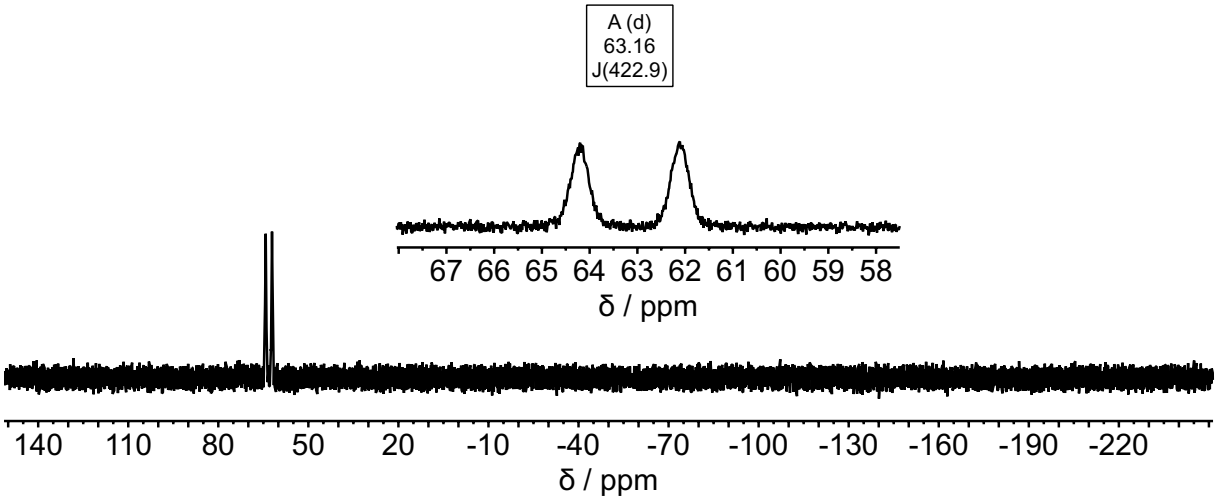

Figure S28. ^{31}P NMR spectrum of **5** in C_6D_6 (202 MHz, 298K).

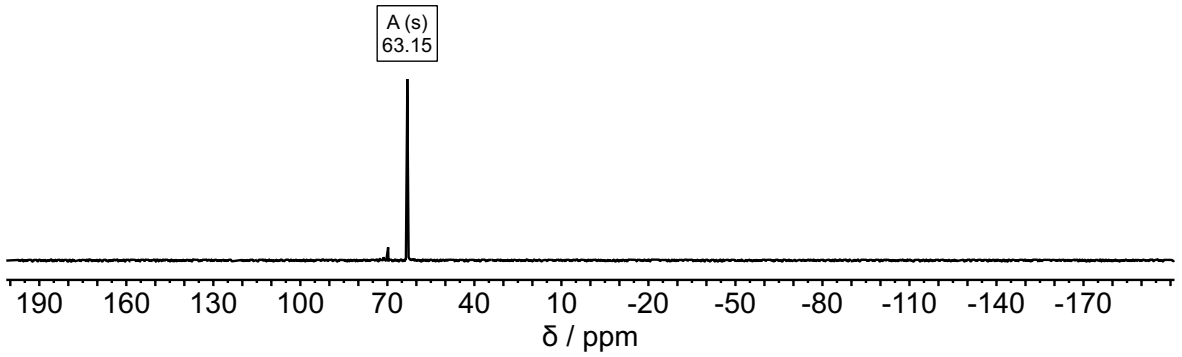

Figure S29. $^{31}P\{^{1}H\}$ NMR spectrum of **5** in C_6D_6 (202 MHz, 298K).

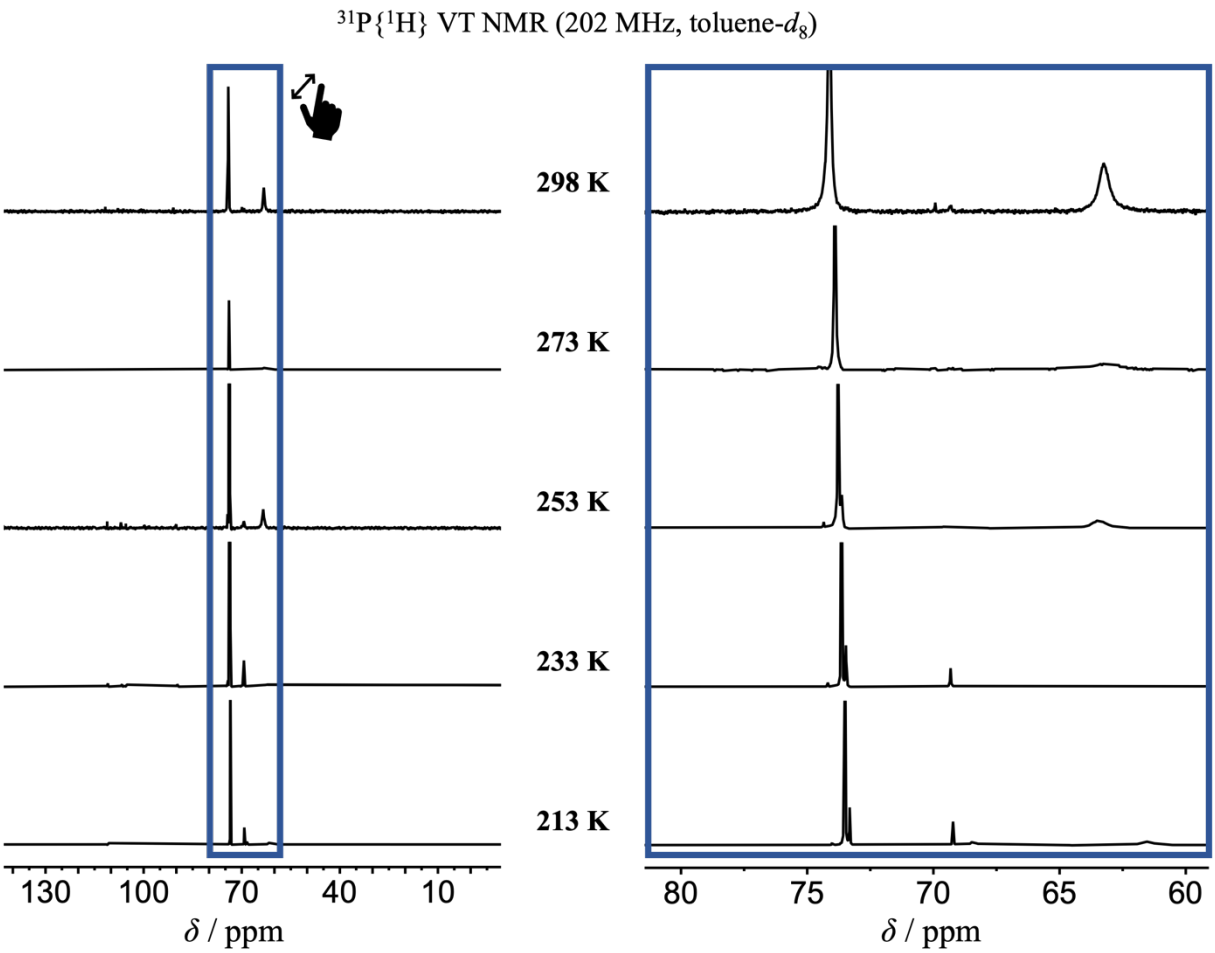

Figure S30. $^{31}P\{^{1}H\}$ VT NMR spectra of a mixture of $Bis_2Ga–O–P^tBu_2{\cdot}EC$ (**3**) and compound **5** recorded in the range between 213 and 298 K in toluene-d_8 (202 MHz).

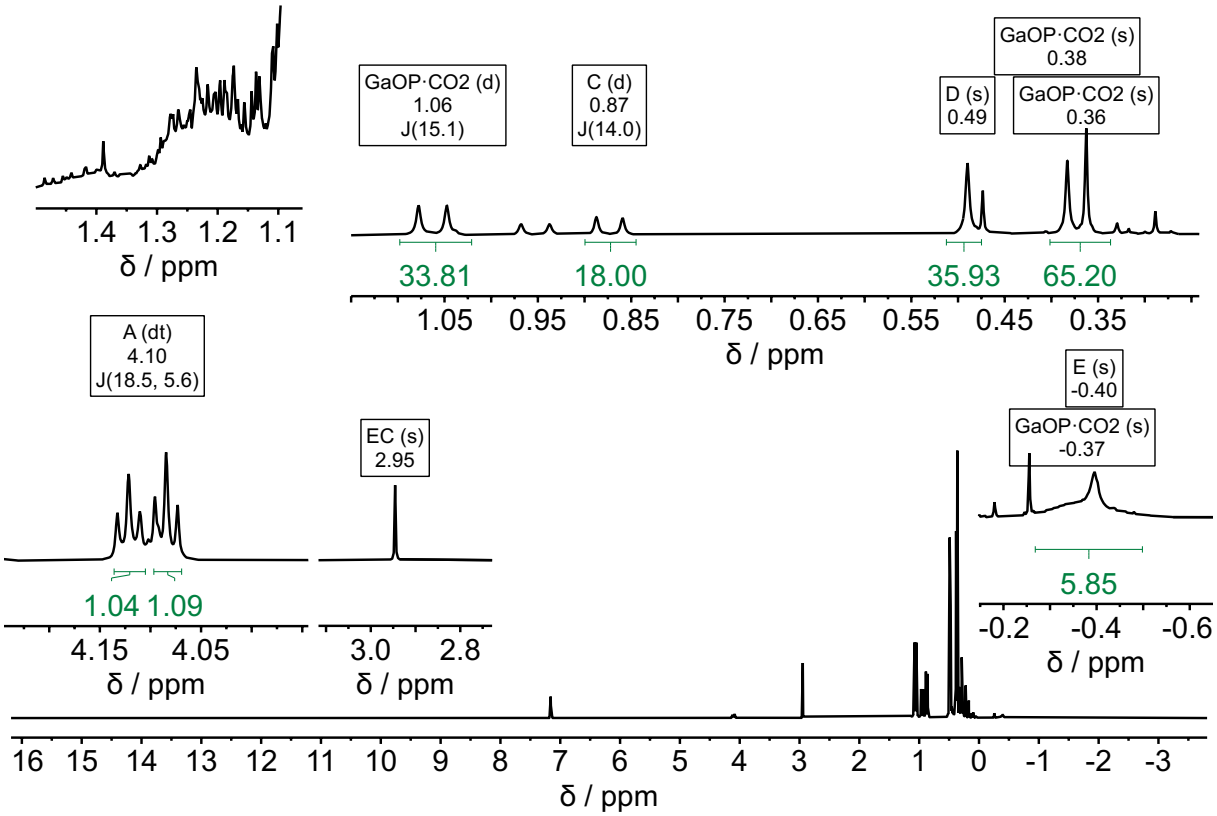

Figure S31. ^{1}H NMR spectrum Bis$_2$Ga–O–P^{t}Bu$_2$·CO$_2$ (**6**) and Bis$_2$Ga–O–P^{t}Bu$_2$·EO (**7**) plus EC in C_6D_6 (500 MHz, 298K). For **7**: *δ* [ppm] = –0.40 (br. s, 2H, GaC**H**), 0.49 (s, 36H, Si(C**H**$_3$)$_3$), 0.87 (d, $^3J_{P,H}$ = 14.0 Hz, 18H, C(C**H**$_3$)$_3$), 4.10 (dt, $^3J_{P,H}$ = 18.5 Hz, $^3J_{H,H}$ = 5.6 Hz, 2H, OC**H**$_2$); due to overlapping resonances, as well in 2D spectra, signals for PC**H**$_2$ could not be localized exactly.

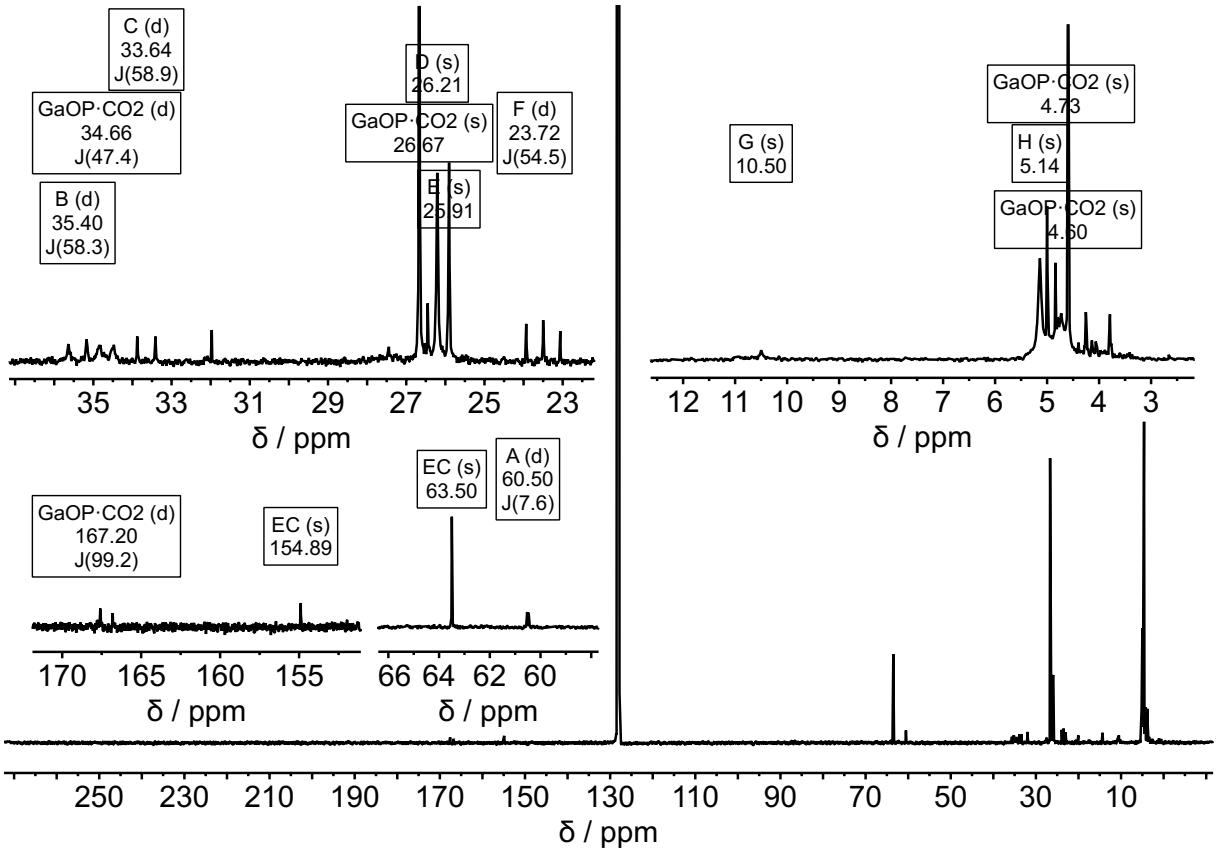

Figure S32. $^{13}C\{^{1}H\}$ NMR spectrum of $Bis_2Ga–O–P^tBu_2·CO_2$ (**6**) and $Bis_2Ga–O–P^tBu_2·EO$ (**7**) plus EC in C_6D_6 (126 MHz, 298K). For **7**: δ [ppm] = 5.1 (s, Si(**C**$H_3)_3$), 10.5 (s, Ga**C**H), 23.7 (d, $^1J_{P,C}$ = 54.5 Hz, P**C**H_2), 25.9 (s, C(**C**$H_3)_3$), 26.2 (s, C(**C**$H_3)_3$), 33.6 (d, $^1J_{P,C}$ = 58.9 Hz, **C**$(CH_3)_3$), 35.4 (d, $^1J_{P,C}$ = 58.3 Hz, **C**$(CH_3)_3$), 60.5 (d, $^2J_{P,C}$ = 7.6 Hz, O**C**H_2).

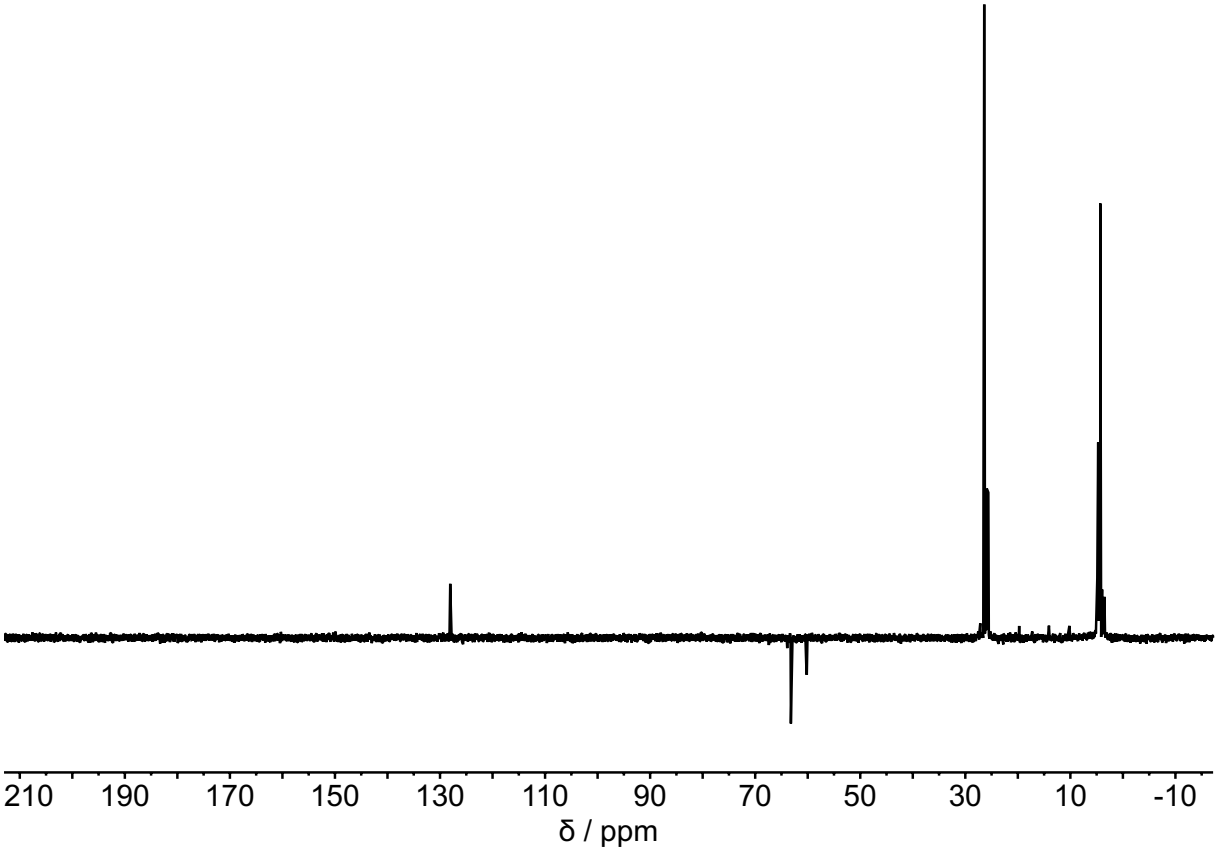

Figure S33. ^{13}C DEPT-135 NMR spectrum of $Bis_2Ga–O–P^tBu_2·CO_2$ (**6**) and $Bis_2Ga–O–P^tBu_2·EO$ (**7**) plus EC in C_6D_6 (126 MHz, 298K).

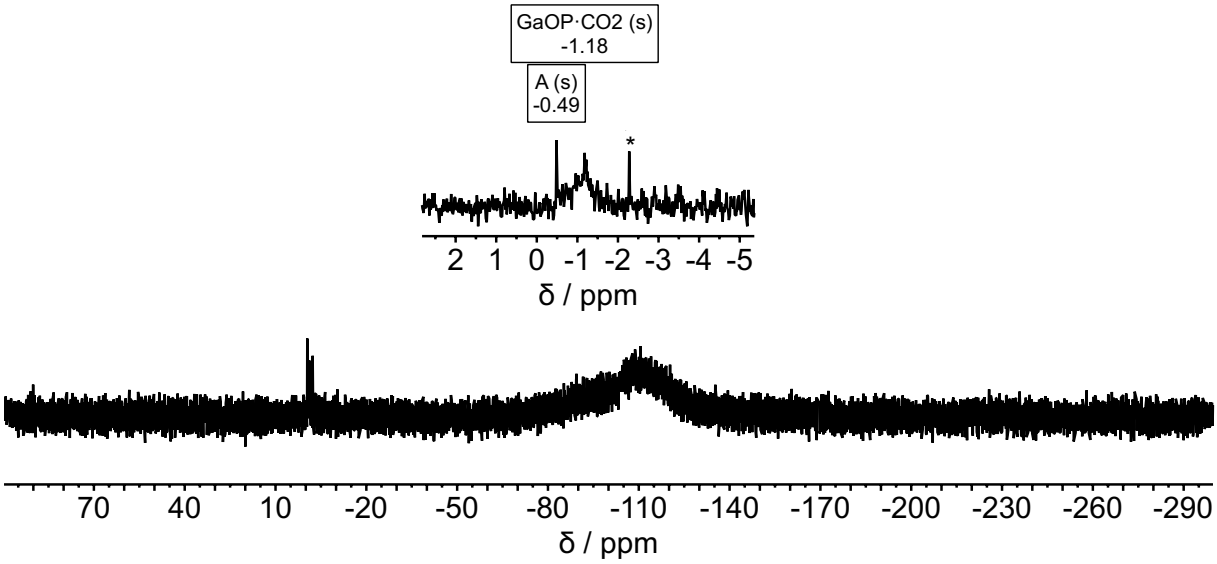

Figure S34. $^{29}Si\{^1H\}$ NMR spectrum of $Bis_2Ga–O–P^tBu_2·CO_2$ (**6**) and $Bis_2Ga–O–P^tBu_2·EO$ (**7**) in C_6D_6 (99 MHz, 298K). For **7**: δ [ppm] = –0.5 (s). The signal denoted with * results from partial hydrolysis (Bis_2GaOH).

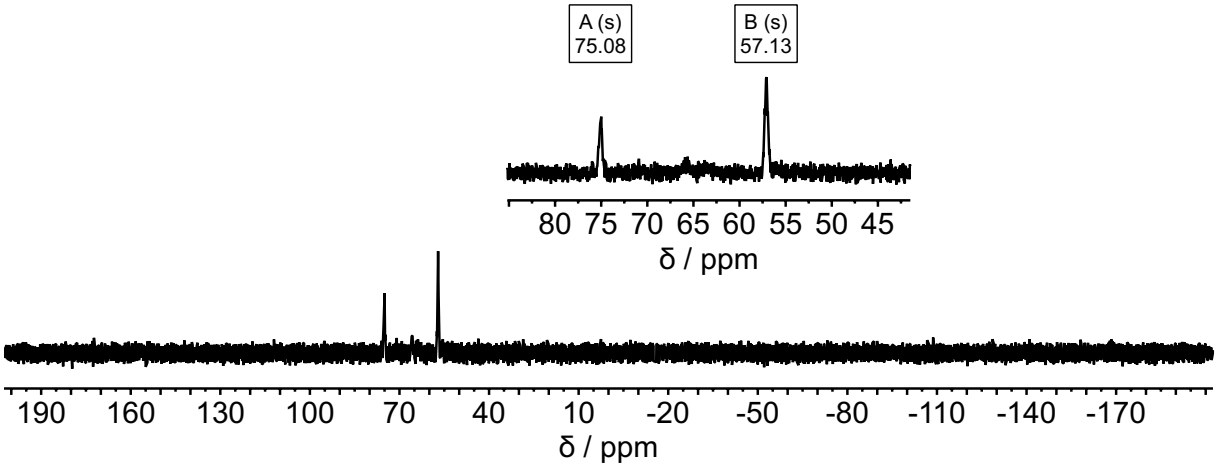

Figure S35. ^{31}P NMR spectrum of $Bis_2Ga–O–P^tBu_2·CO_2$ (**6**) and $Bis_2Ga–O–P^tBu_2·EO$ (**7**) in C_6D_6 (202 MHz, 298K). For **7**: δ [ppm] = 75.1 (s).

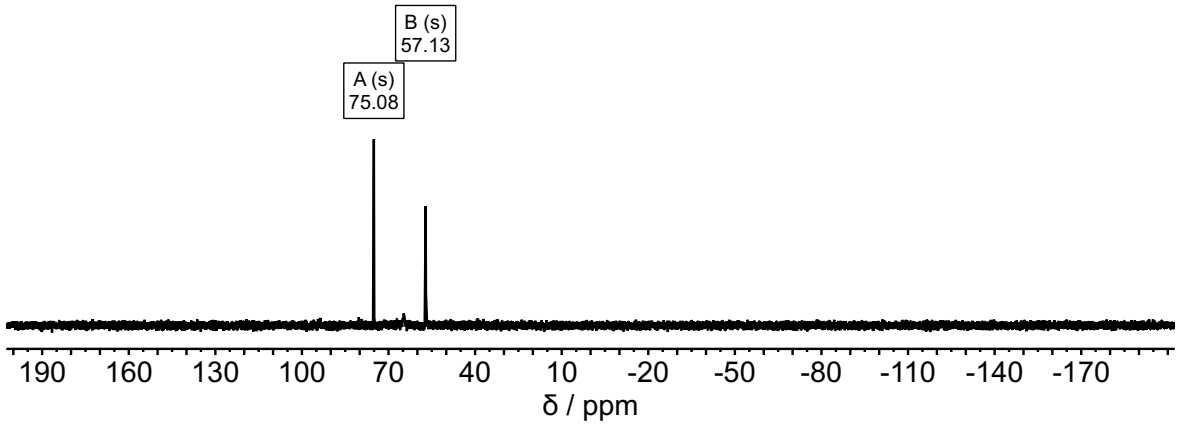

Figure S36. ^{31}P{^{1}H} NMR spectrum of $Bis_2Ga–O–P^tBu_2·CO_2$ (**6**) and $Bis_2Ga–O–P^tBu_2·EO$ (**7**) in C_6D_6 (202 MHz, 298K). For **7**: δ [ppm] = 75.1 (s).

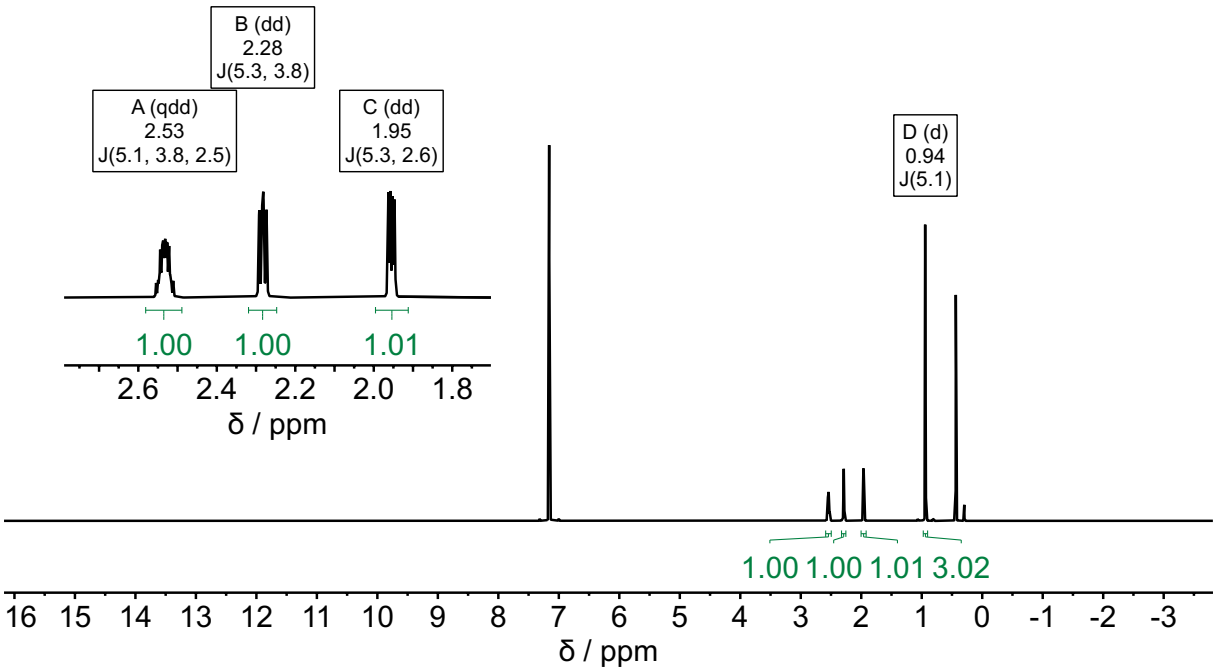

Figure S37. ^{1}H NMR spectrum of propylene oxide (PO) in C_6D_6 (500 MHz, 298K).

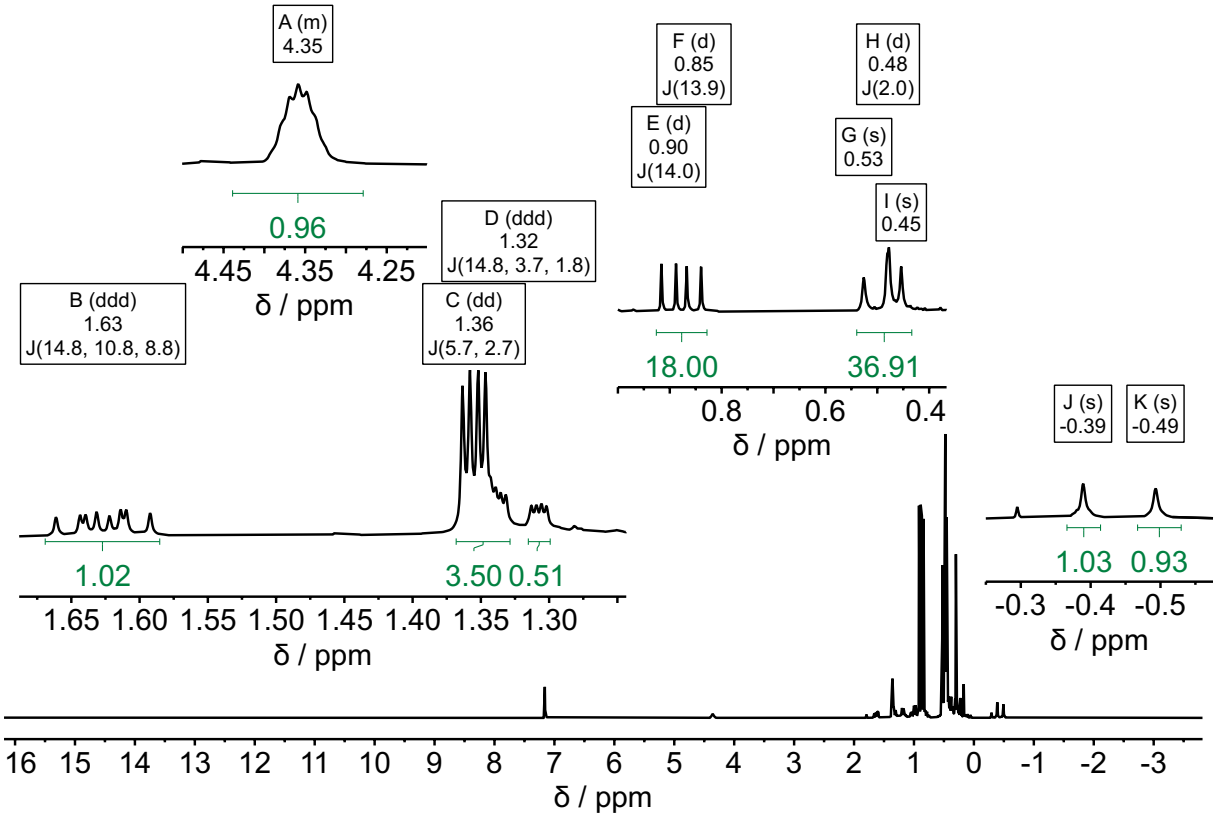

Figure S38. ^{1}H NMR spectrum of Bis$_2$Ga–O–P^{t}Bu$_2$·PO (**8**) in C_6D_6 (500 MHz, 298K): δ [ppm] = –0.49 (s, 1H, GaC**H**), –0.39 (s, 1H, GaC**H**), 0.42 – 0.56 (m, 36H, Si(C**H**$_3$)$_3$), 0.85 (d, $^{3}J_{P,H}$ = 13.9 Hz, 9H, C(C**H**$_3$)$_3$), 0.90 (d, $^{3}J_{P,H}$ = 14.0 Hz, 9H, C(C**H**$_3$)$_3$), 1.32 (ddd, J =14.8, 3.7, 1.8 Hz, PC**H**$_2$), 1.36 (dd, J =5.7, 2.7 Hz, C**H**$_3$), 1.63 (ddd, J =14.8, 10.8, 8.8 Hz, PC**H**$_2$), 4.35 (m, 1H, OC**H**).

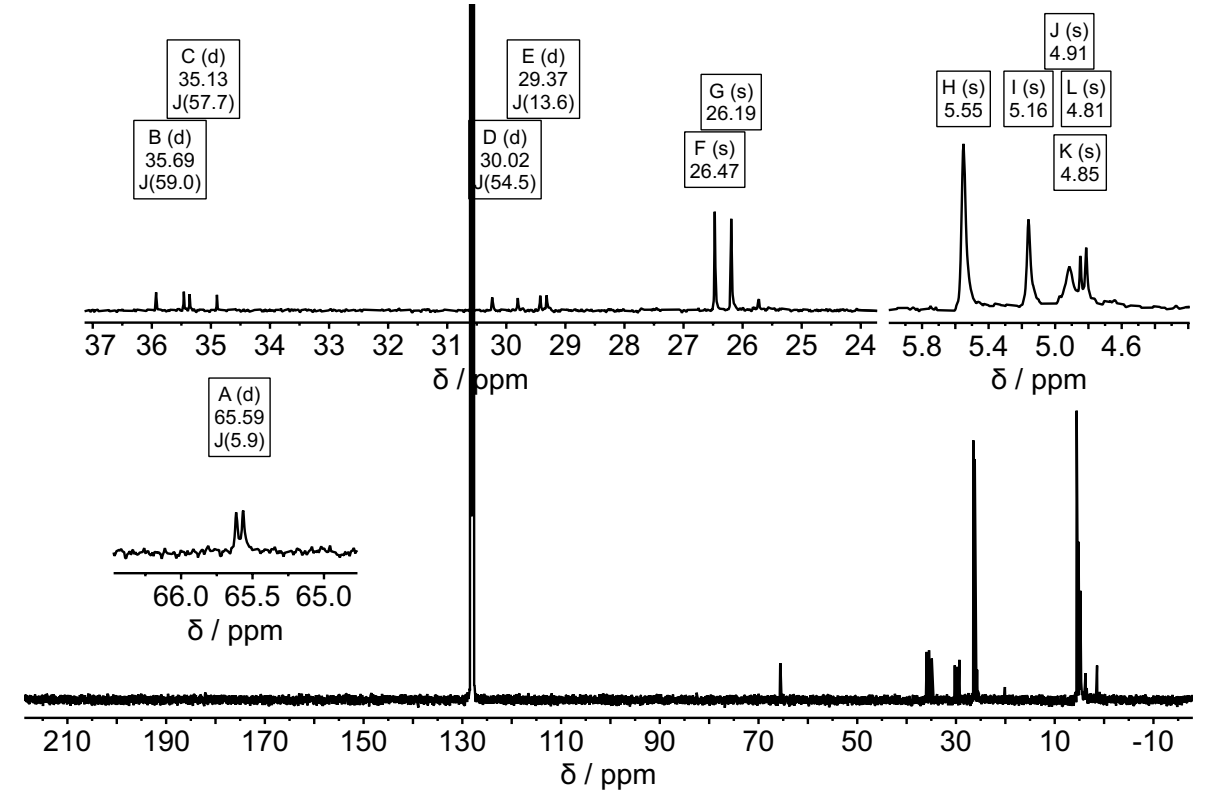

Figure S39. ^{13}C{^{1}H} NMR spectrum of Bis$_2$Ga–O–P^{t}Bu$_2$·PO (**8**) in C_6D_6 (126 MHz, 298K): δ [ppm] = 4.8 (s, overlapped, from ^{1}H-^{13}C HSQC experiment, Ga**C**H), 4.9 (s, Si(**C**H$_3$)$_3$), 5.2 (s, Si(**C**H$_3$)$_3$), 5.6 (s, Si(**C**H$_3$)$_3$), 5.6

(s, overlapped, from ^{1}H-^{13}C HSQC experiment, Ga**C**H), 26.2 (s, C(**C**H$_3$)$_3$), 26.5 (s, C(**C**H$_3$)$_3$), 29.4 (d, $^{3}J_{P,C}$ = 13.6 Hz, **C**H$_3$), 30.0 (d, $^{1}J_{P,C}$ = 54.5 Hz, P**C**H$_2$), 35.1 (d, $^{1}J_{P,C}$ = 57.7 Hz, **C**(CH$_3$)$_3$), 35.7 (d, $^{1}J_{P,C}$ = 59.0 Hz, **C**(CH$_3$)$_3$), 65.6 (d, $^{2}J_{P,C}$ = 5.9 Hz, O**C**H).

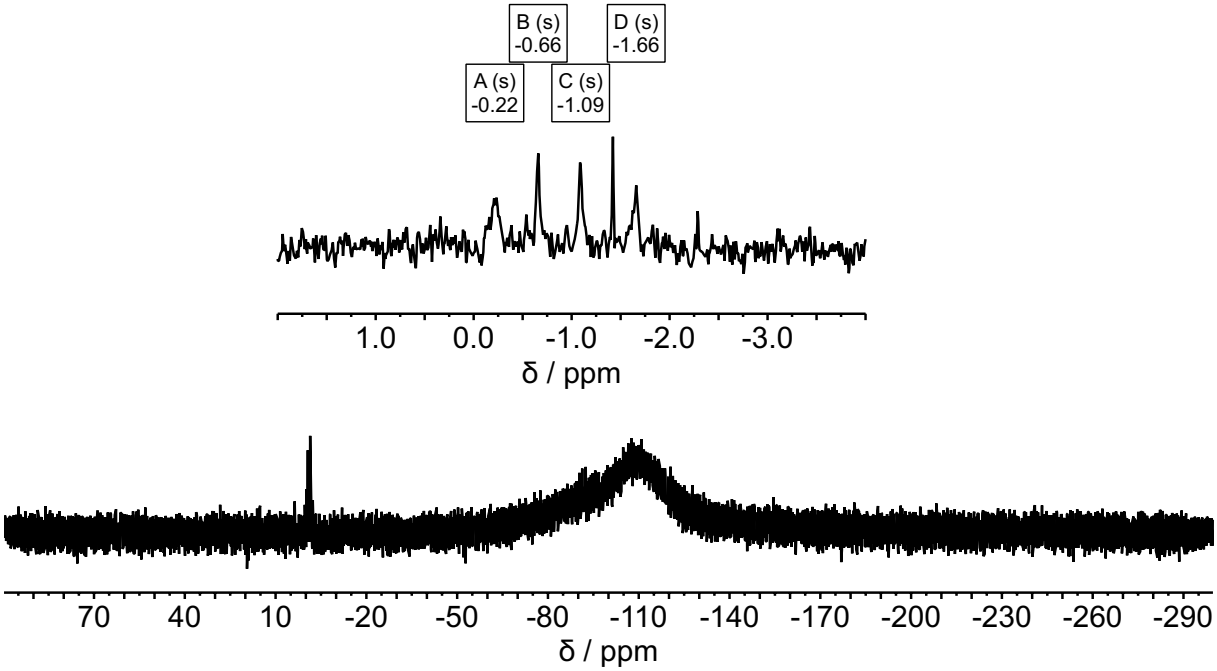

Figure S40. ^{29}Si{^{1}H} NMR spectrum of Bis$_2$Ga–O–P^{t}Bu$_2$·PO (**8**) in C$_6$D$_6$ (99 MHz, 298K).

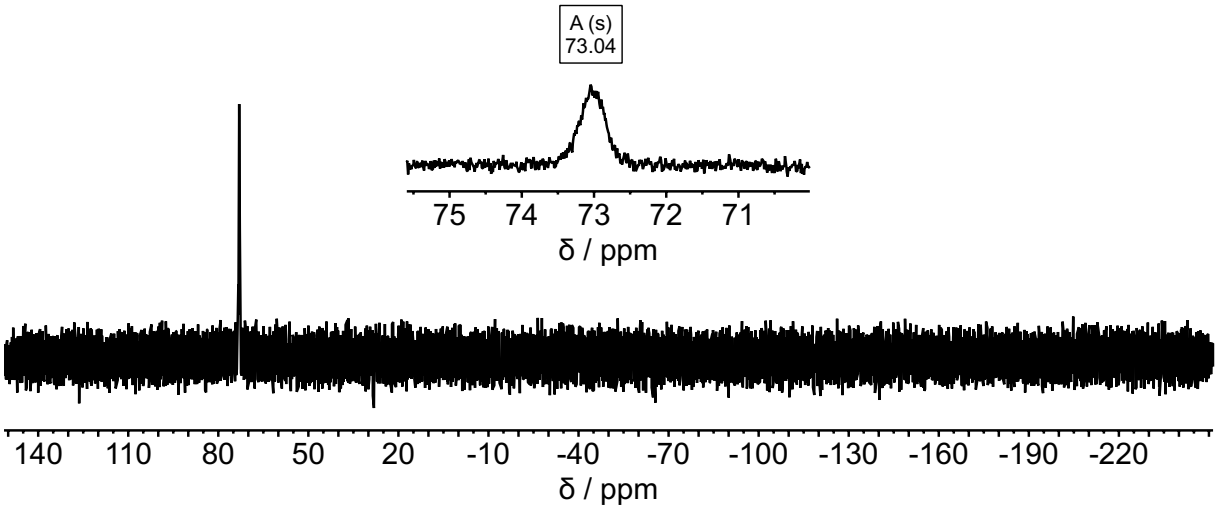

Figure S41. ^{31}P NMR spectrum of Bis$_2$Ga–O–P^{t}Bu$_2$·PO (**8**) in C$_6$D$_6$ (202 MHz, 298K).

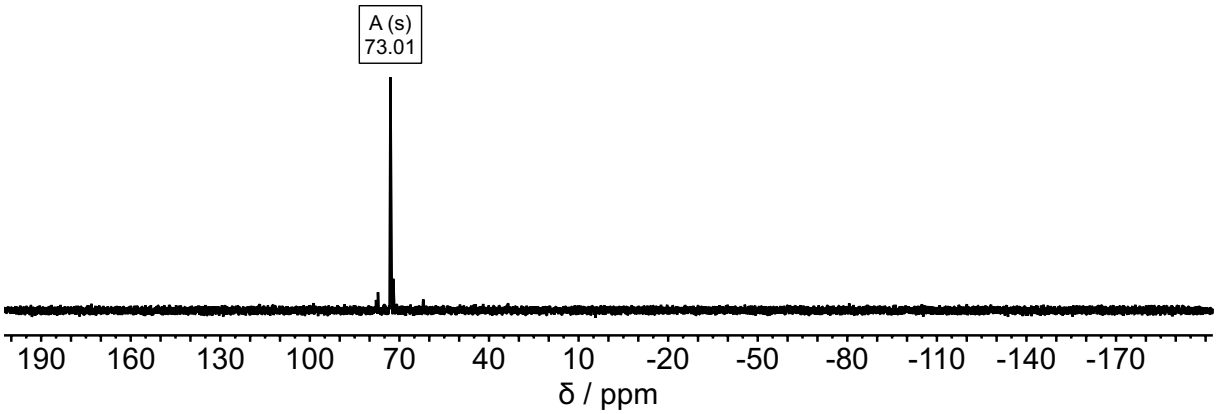

Figure S42. ^{31}P{^{1}H} NMR spectrum of Bis$_2$Ga–O–P^{t}Bu$_2$·PO (**8**) in C$_6$D$_6$ (202 MHz, 298K).

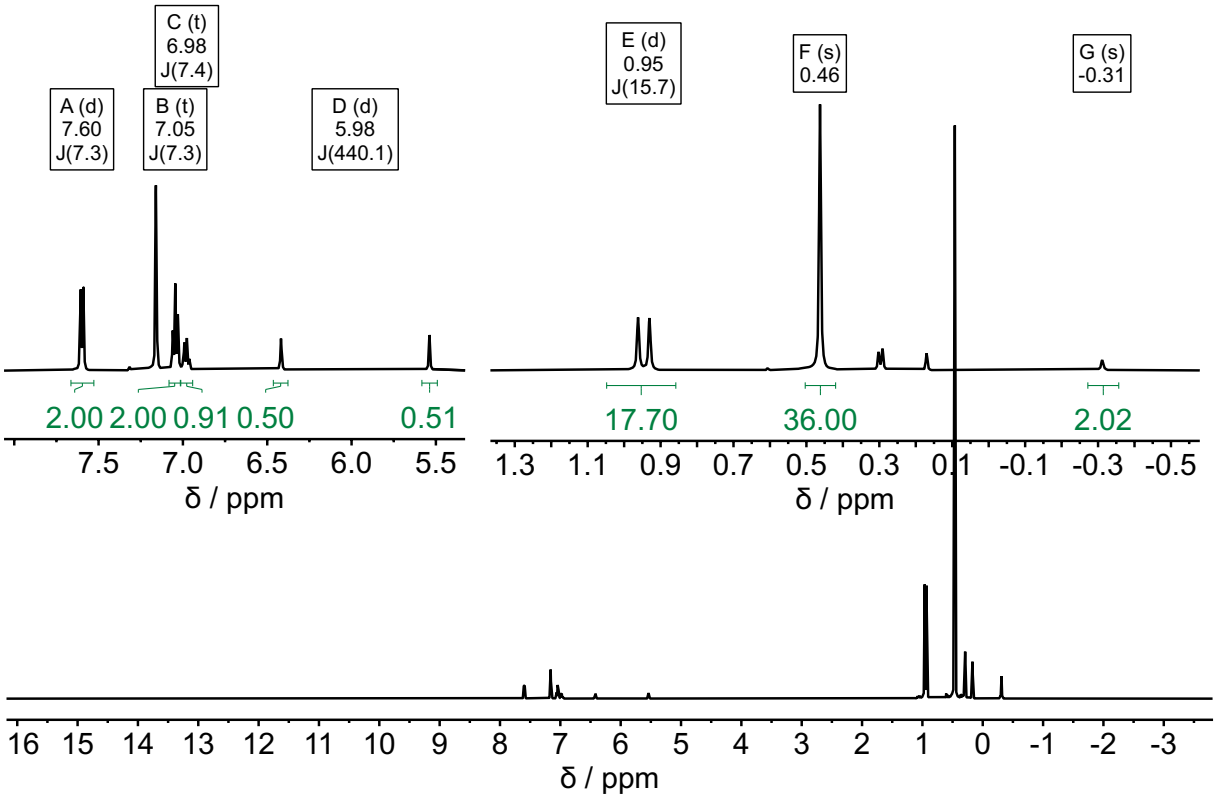

Figure S43. ^{1}H NMR spectrum of Bis$_2$Ga–O–P^{t}Bu$_2$·PhC≡CH as the deprotonation adduct (**9a**) in C_6D_6 (500 MHz, 298K): δ [ppm] = –0.31 (s, 2H, GaC**H**), 0.46 (s, 36H, Si(C**H**$_3$)$_3$), 0.95 (d, $^{3}J_{P,H}$ = 15.7 Hz, 18H, C(C**H**$_3$)$_3$), 5.98 (d, $^{1}J_{P,H}$ = 440.1 Hz, 1H, P**H**), 6.98 (t, $^{3}J_{H,H}$ = 7.4 Hz, 1H, *para*-**H**), 7.05 (t, $^{3}J_{H,H}$ = 7.3 Hz, 2H, *meta*-**H**), 7.62 (d, $^{3}J_{H,H}$ = 7.8 Hz, 2H, *ortho*-**H**).

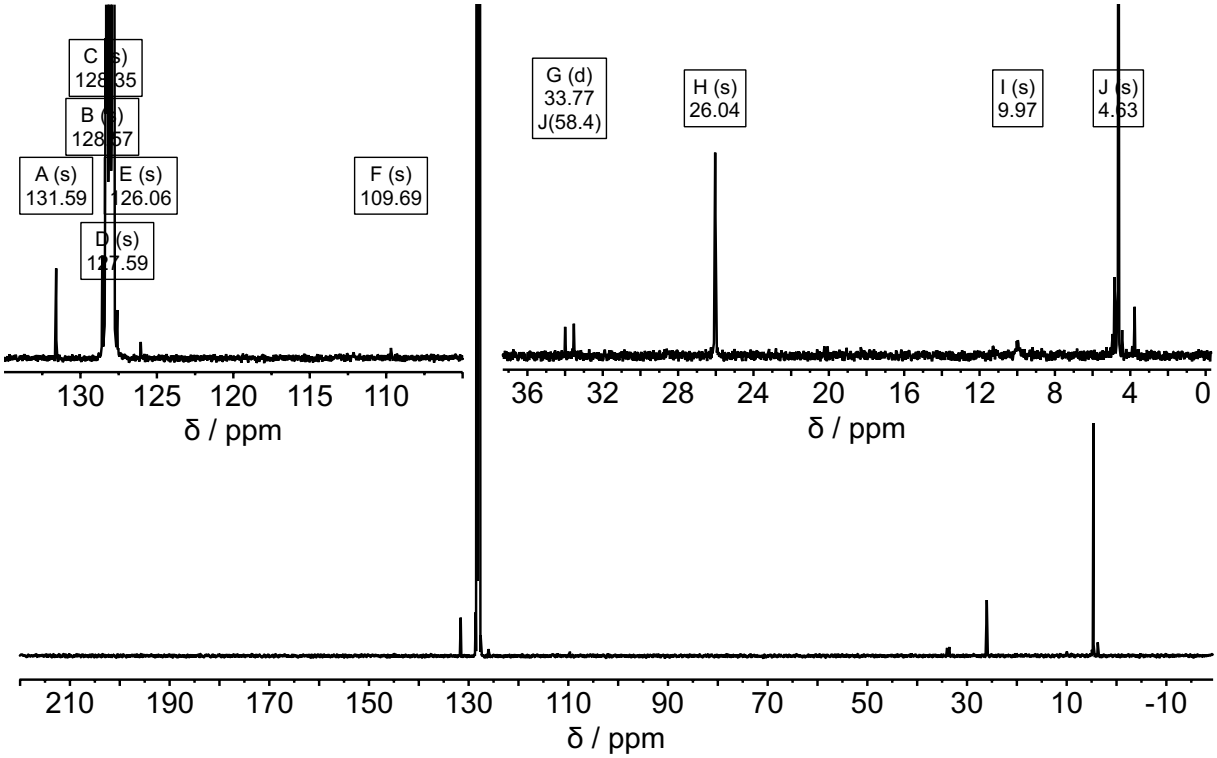

Figure S44. ^{13}C{^{1}H} NMR spectrum of Bis$_2$Ga–O–P^{t}Bu$_2$·PhC≡CH as the deprotonation adduct (**9a**) in C_6D_6 (126 MHz, 298K): δ [ppm] = 4.6 (s, Si(**C**H$_3$)$_3$), 10.0 (s, Ga**C**H), 26.0 (s, C(**C**H$_3$)$_3$), 33.8 (d, $^{1}J_{P,C}$ = 58.4 Hz, **C**(CH$_3$)$_3$), 109.7 (s, PhC≡**C**Ga), 126.1 (s, Ph**C**≡CGa), 127.6 (s, *para*-**C**), 128.4 (s, *ipso*-**C**), 128.6 (s, *meta*-**C**), 131.6 (s, *ortho*-**C**).

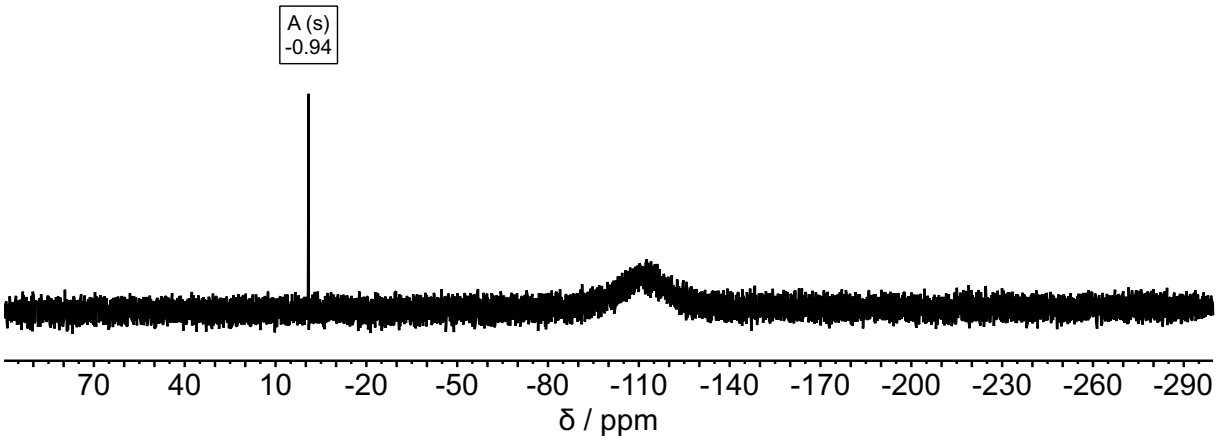

Figure S45. $^{29}Si\{^{1}H\}$ NMR spectrum of $Bis_2Ga–O–P^tBu_2·PhC≡CH$ as the deprotonation adduct (**9a**) in C_6D_6 (99 MHz, 298K).

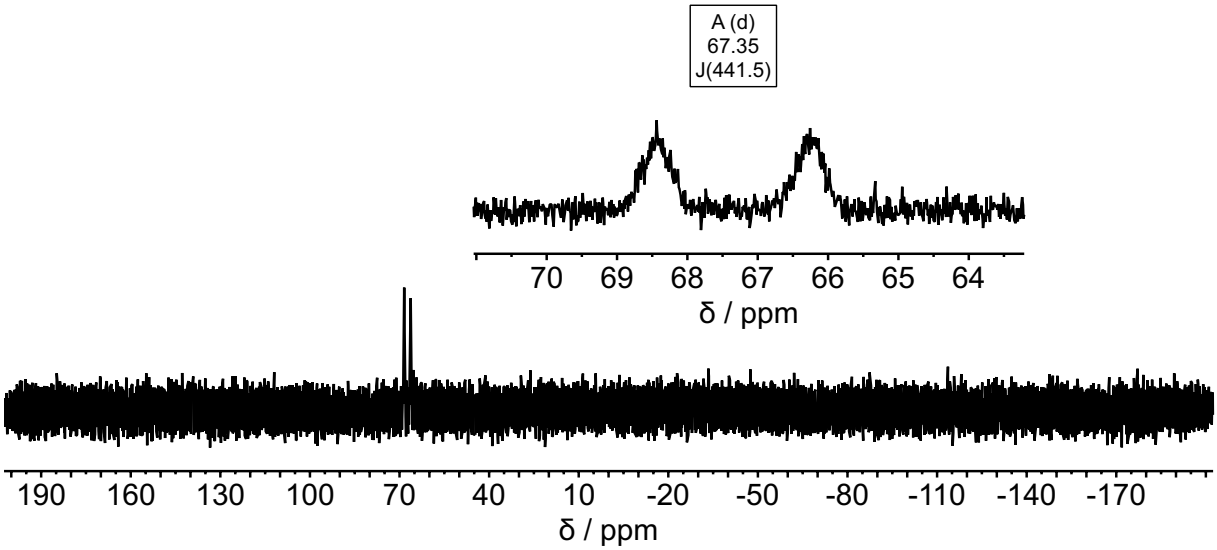

Figure S46. ^{31}P NMR spectrum of $Bis_2Ga–O–P^tBu_2·PhC≡CH$ as the deprotonation adduct (**9a**) in C_6D_6 (202 MHz, 298K).

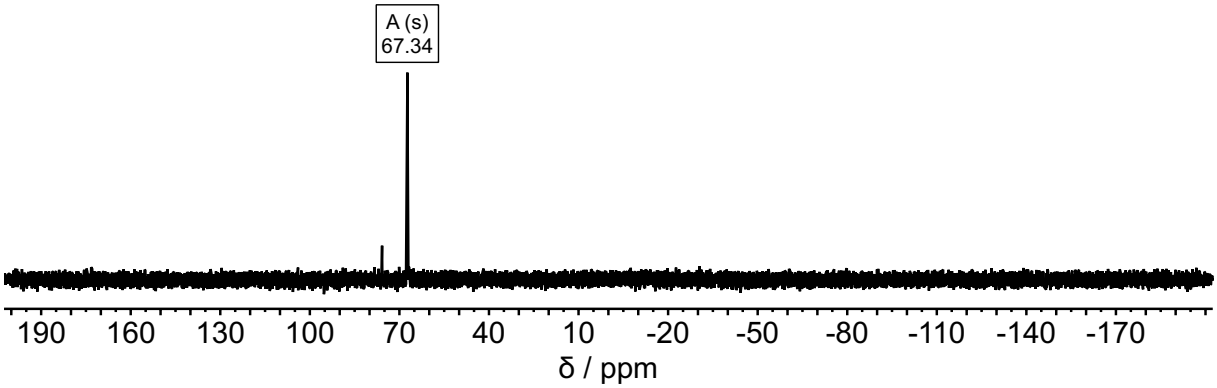

Figure S47. $^{31}P\{^{1}H\}$ NMR spectrum of $Bis_2Ga–O–P^tBu_2·PhC≡CH$ as the deprotonation adduct (**9a**) in C_6D_6 (202 MHz, 298K).

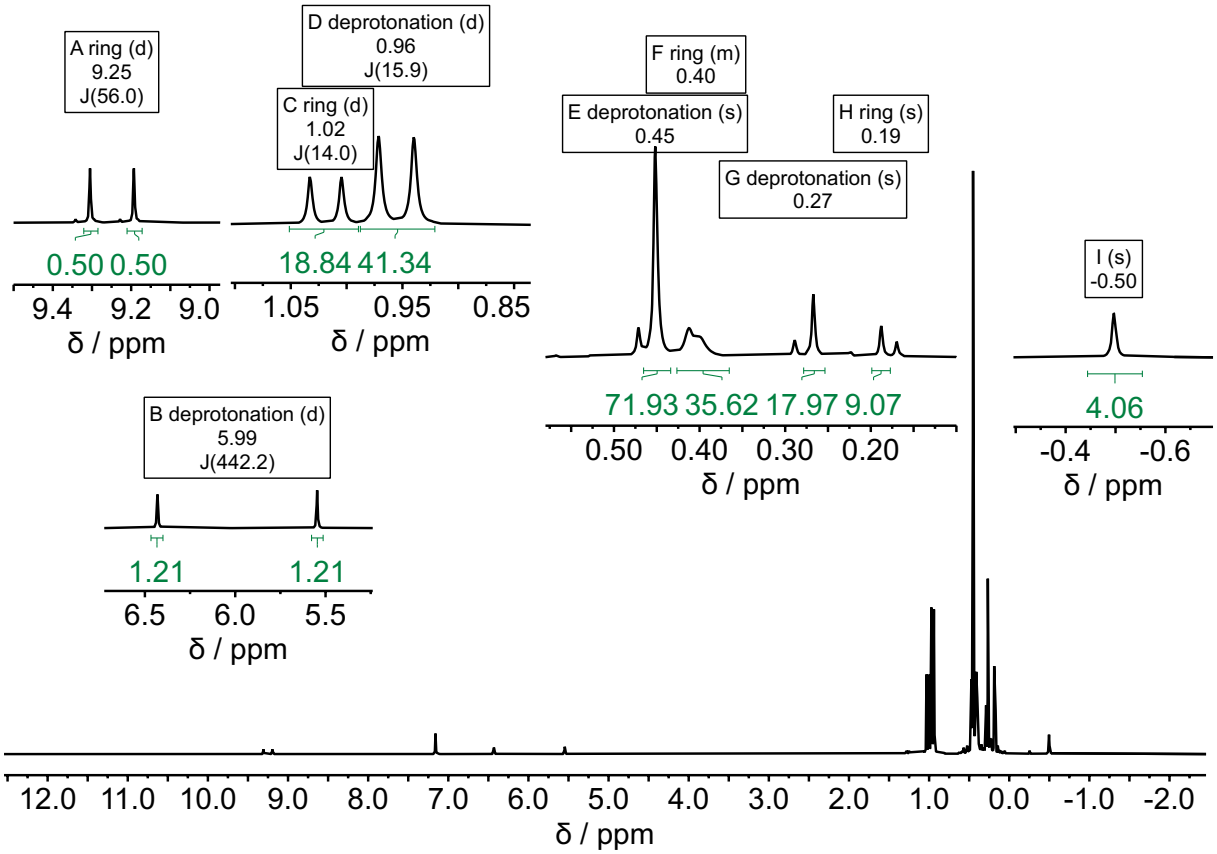

Figure S48. ^{1}H NMR spectrum of Bis$_2$Ga–O–P^{t}Bu$_2$·Me$_3$SiC≡CH (**10**) as a mixture of deprotonation (**10a**) and ring-closure product (**10b**) in C_6D_6 (500 MHz, 298K). For **10a:** δ [ppm] = –0.50 (s, 2H, GaC**H**), 0.27 (s, 9H, Si(C**H**$_3$)$_3$), 0.46 (s, 36H, CH(Si(C**H**$_3$)$_3$)$_2$), 0.96 (d, $^{3}J_{P,H}$ = 15.6 Hz, 18H, C(C**H**$_3$)$_3$), 5.97 (d, $^{1}J_{P,H}$ = 442.2 Hz, 1H, P**H**). For **10b**: δ [ppm] = –0.50 (br. s, 2H, GaC**H**), 0.18 (s, 9H, Si(C**H**$_3$)$_3$), 0.38 – 0.43 (s, 36H, CH(Si(C**H**$_3$)$_3$)$_2$), 1.02 (d, $^{3}J_{P,H}$ = 14.0 Hz, 18H, C(C**H**$_3$)$_3$), 9.25 (d, $^{3}J_{P,H}$ = 56.0 Hz, 1H, PC**H**).

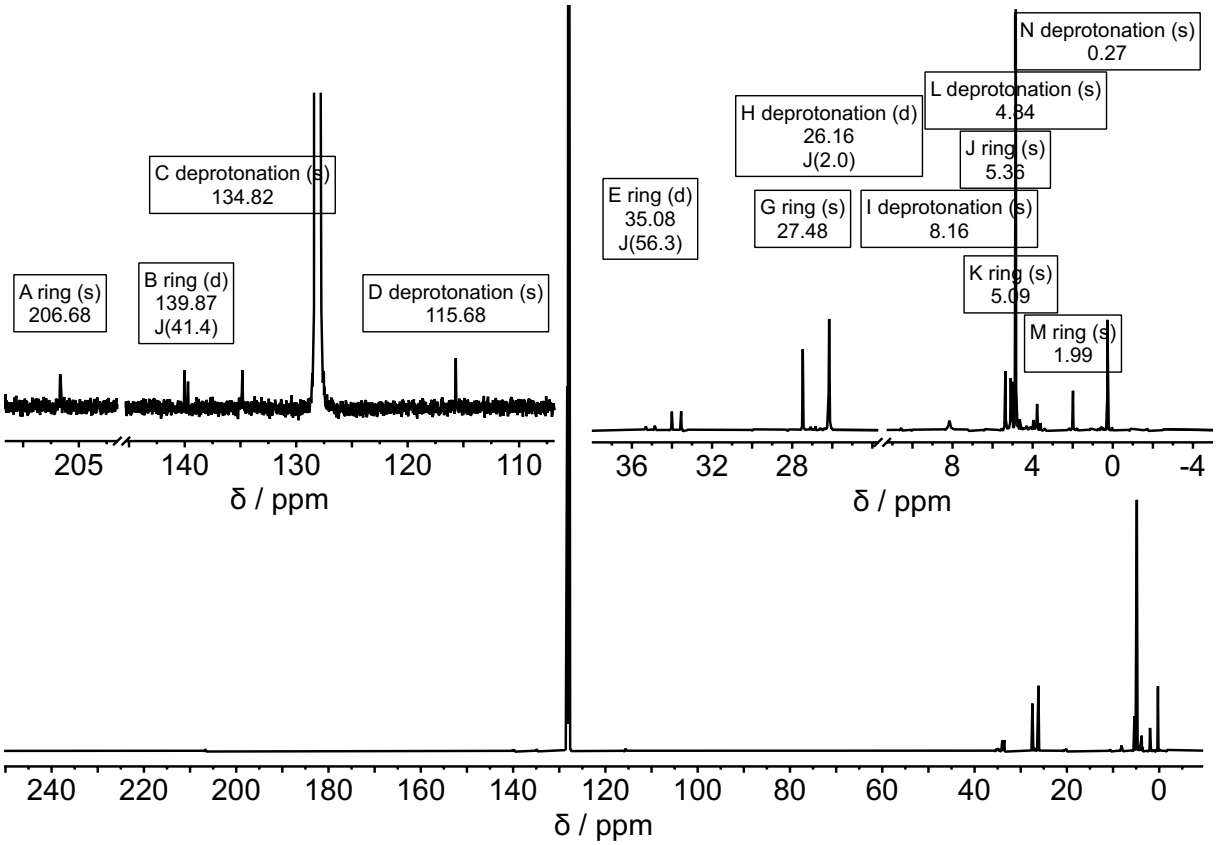

Figure S49. $^{13}C\{^{1}H\}$ NMR spectrum of $Bis_2Ga–O–P^tBu_2·Me_3SiC{\equiv}CH$ (**10**) as a mixture of deprotonation (**10a**) and ring-closure product (**10b**) in C_6D_6 (126 MHz, 298K). For **10a:** δ [ppm] = 0.3 (s, Si(**C**$H_3)_3$), 4.8 (s, Si(**C**$H_3)_3$), 8.2 (s, Ga**C**H), 26.2 (s, C(**C**$H_3)_3$), 33.8 (d, $^{1}J_{P,C}$ = 58.3 Hz, **C**$(CH_3)_3$), 115.7 (s, $Me_3SiC{\equiv}$**C**Ga), 134.8 (s, Me_3Si**C**≡CGa).For **10b**: δ [ppm] = 2.0 (s, Si(**C**$H_3)_3$), 5.1/5.4 (s, Si(**C**$H_3)_3$), 27.5 (s, C(**C**$H_3)_3$), 35.1 (d, $^{1}J_{P,C}$ = 56.3 Hz, **C**$(CH_3)_3$), 139.9 (d, $^{1}J_{P,C}$ = 41.4 Hz, GaC=**C**P), 206.7 (d, $^{2}J_{P,C}$ = 5.9 Hz, Ga**C**=CP); a signal for Ga**C**H could not be observed.

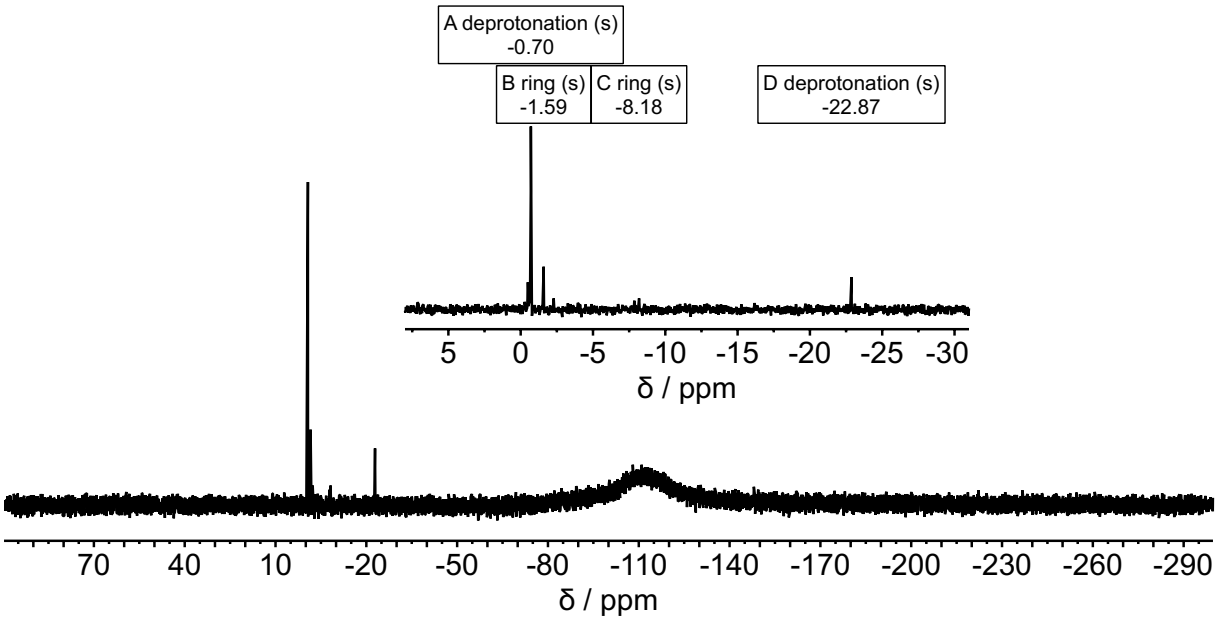

Figure S50. $^{29}Si\{^{1}H\}$ NMR spectrum of $Bis_2Ga–O–P^tBu_2·Me_3SiC{\equiv}CH$ (**10**) as a mixture of deprotonation (**10a**) and ring-closure product (**10b**) in C_6D_6 (99 MHz, 298K).

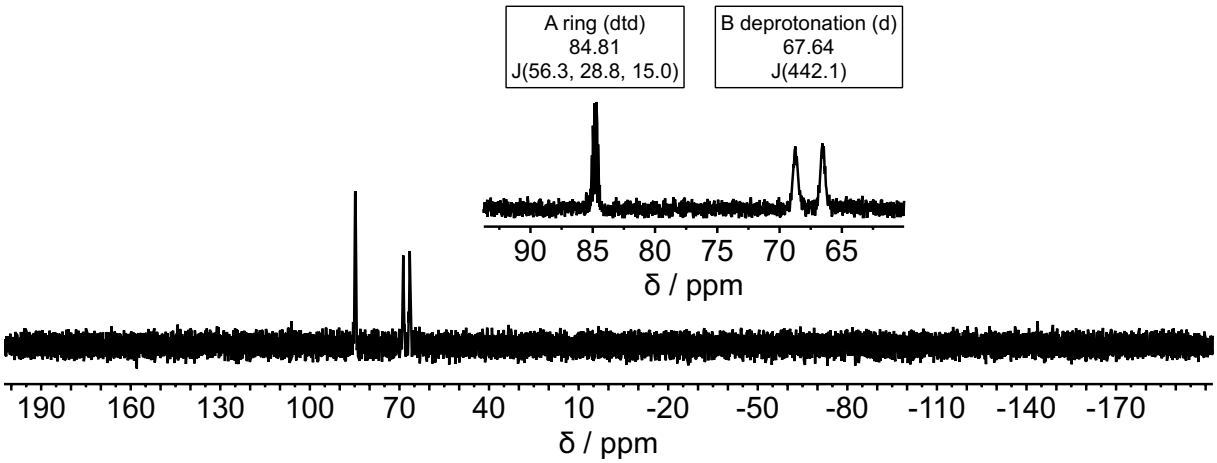

Figure S51. ^{31}P NMR spectrum of $Bis_2Ga–O–P^tBu_2·Me_3SiC≡CH$ (**10**) as a mixture of deprotonation (**10a**) and ring-closure product (**10b**) in C_6D_6 (202 MHz, 298K).

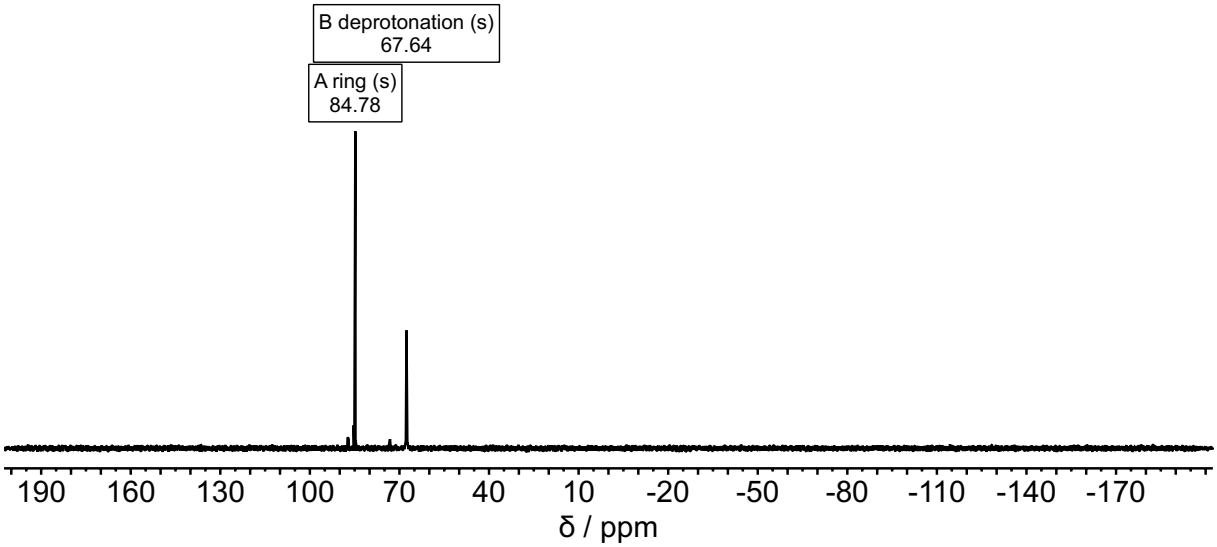

Figure S52. $^{31}P\{^1H\}$ NMR spectrum of $Bis_2Ga–O–P^tBu_2·Me_3SiC≡CH$ (**10**) as a mixture of deprotonation (**10a**) and ring-closure product (**10b**) in C_6D_6 (202 MHz, 298K).

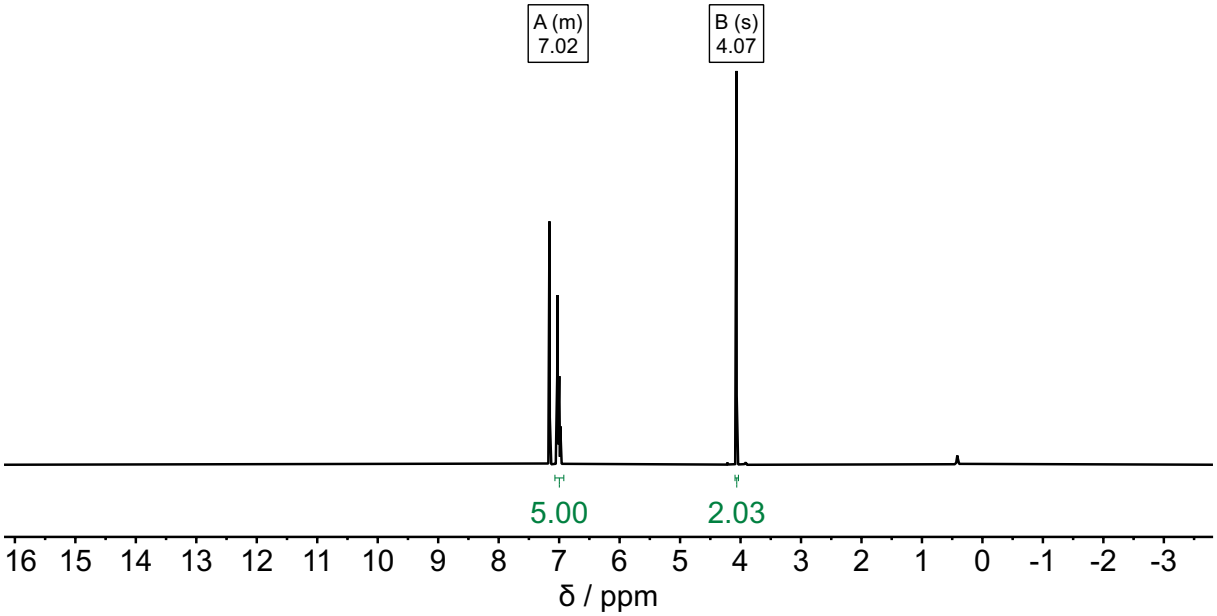

Figure S53. ^1H NMR spectrum of benzyl chloride in C_6D_6 (500 MHz, 298K).

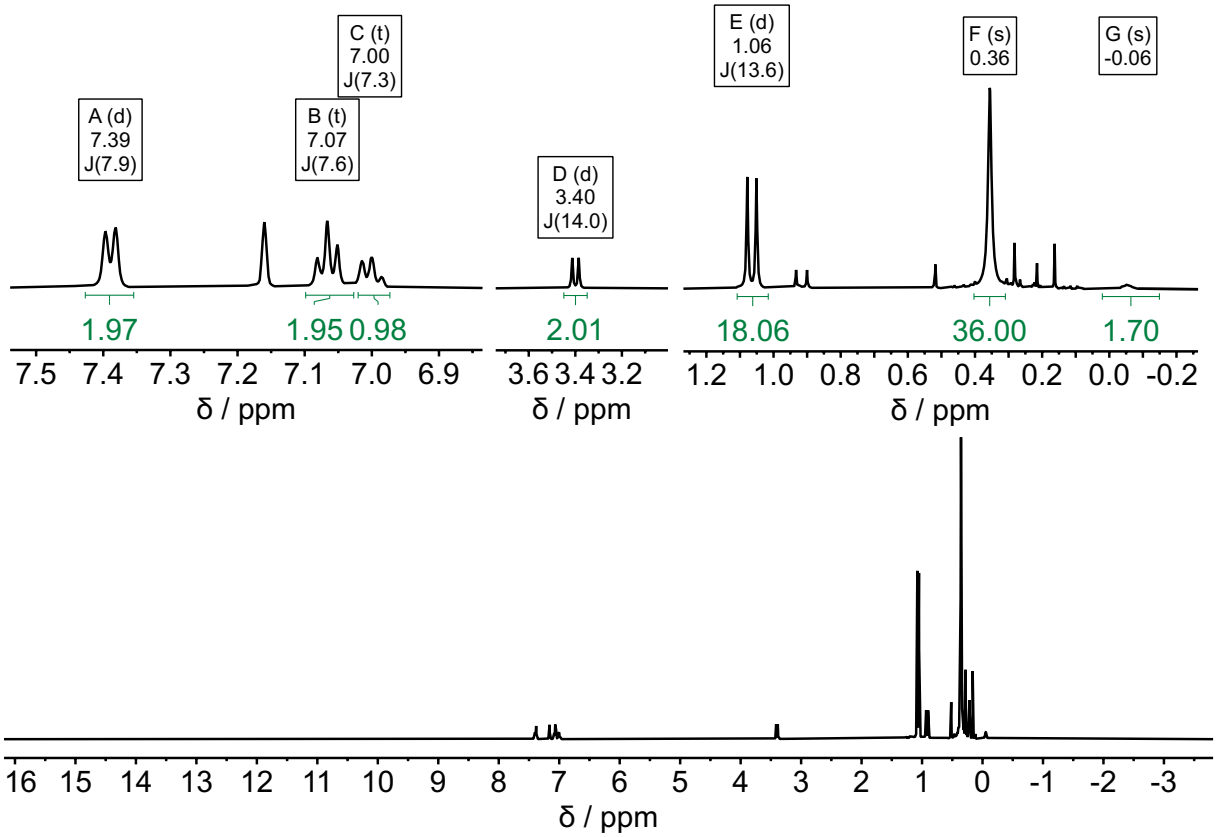

Figure S54. ^{1}H NMR spectrum of $Bis_2(Cl)Ga–O–P(Bn)^tBu_2$ (**11**) in C_6D_6 (500 MHz, 298K): δ [ppm] = –0.06 (s, 2H, GaC**H**), 0.36 (s, 36H, Si(C**H**$_3$)$_3$), 1.06 (d, $^3J_{P,H}$ = 13.6 Hz, 18H, C(C**H**$_3$)$_3$), 3.40 (d, $^3J_{P,H}$ = 14.0 Hz, 2H, C**H**$_2$), 7.00 (t, $^3J_{H,H}$ = 7.3 Hz, 1H, *para*-**H**), 7.05 (t, $^3J_{H,H}$ = 7.6 Hz, 2H, *meta*-**H**), 7.39 (d, $^3J_{H,H}$ = 7.9 Hz, 2H, *ortho*-**H**).

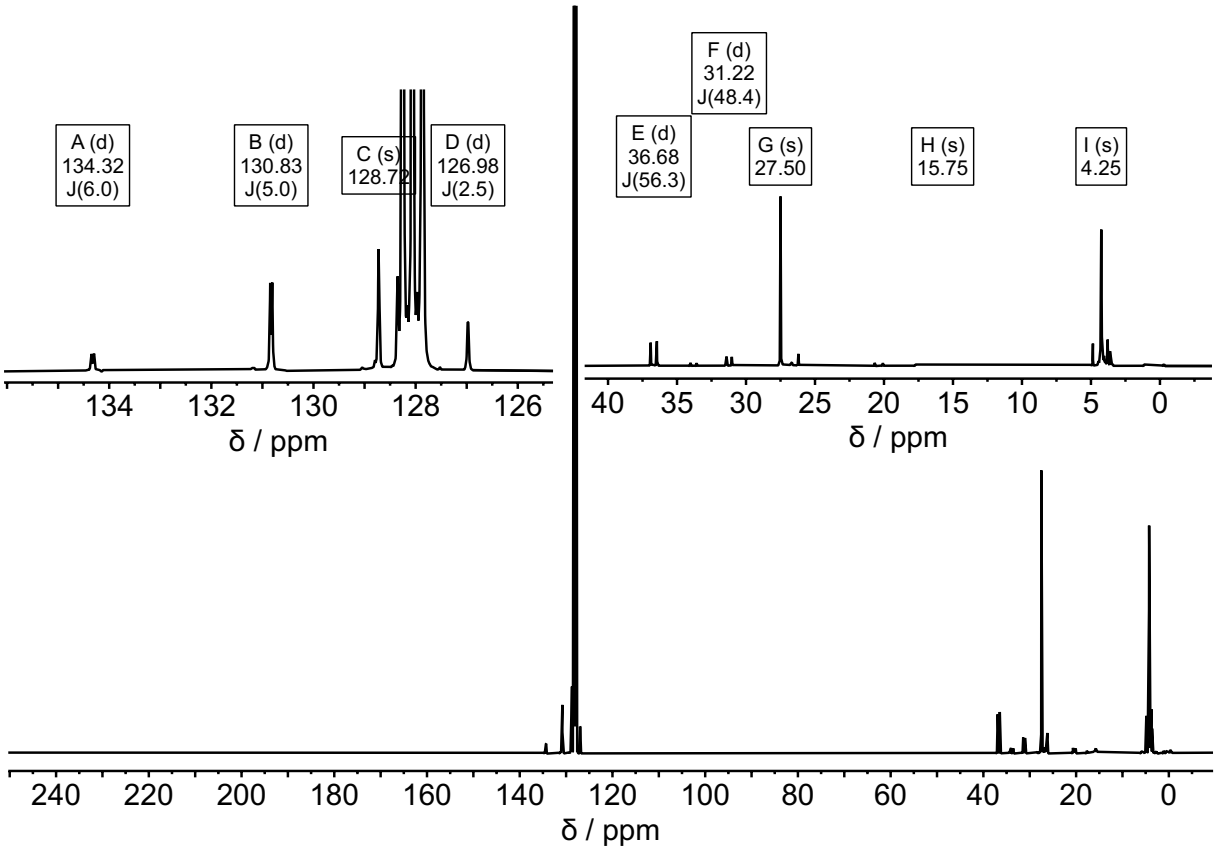

Figure S55. $^{13}C\{^1H\}$ NMR spectrum of $Bis_2(Cl)Ga–O–P(Bn)^tBu_2$ (**11**) in C_6D_6 (126 MHz, 298K): δ [ppm] = 4.3

(s, Si(**C**H$_3$)$_3$), 15.8 (s, Ga**C**H), 27.5 (s, C(**C**H$_3$)$_3$), 31.2 (d, $^1J_{P,C}$ = 48.4 Hz, **C**H$_2$), 36.7 (d, $^1J_{P,C}$ = 56.3 Hz, **C**(CH$_3$)$_3$), 127.0 (d, $^4J_{P,C}$ = 2.5 Hz, *para*-**C**), 128.7 (s, *meta*-**C**), 130.8 (d, $^3J_{P,C}$ = 5.0 Hz, *ortho*-**C**), 134.3 (d, $^2J_{P,C}$ = 6.0 Hz, *ipso*-**C**).

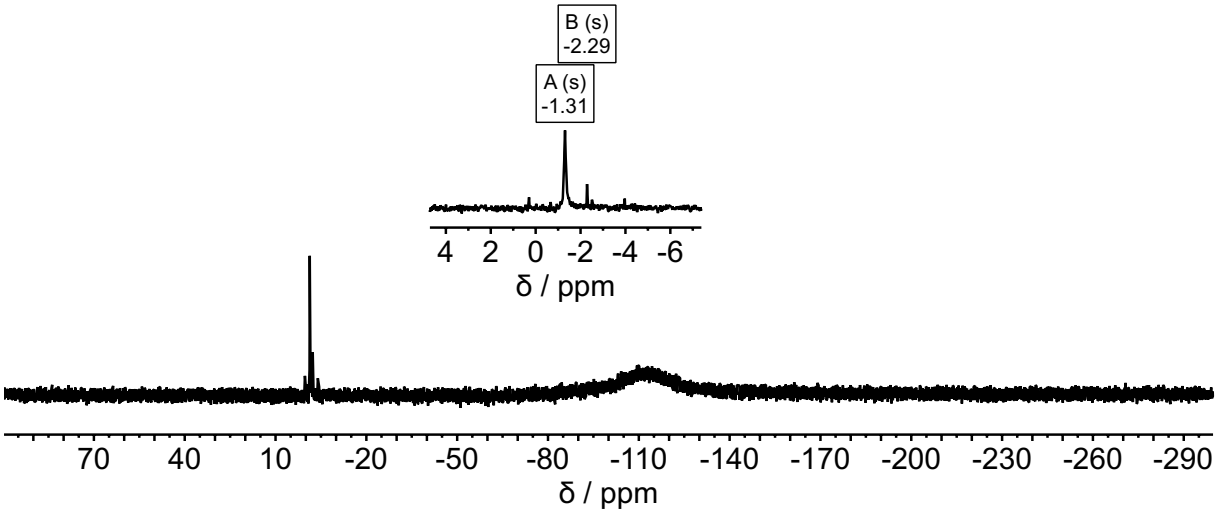

Figure S56. ^{29}Si{^{1}H} NMR spectrum of Bis$_2$(Cl)Ga–O–P(Bn)^{t}Bu$_2$ (**11**) in C$_6$D$_6$ (99 MHz, 298K).

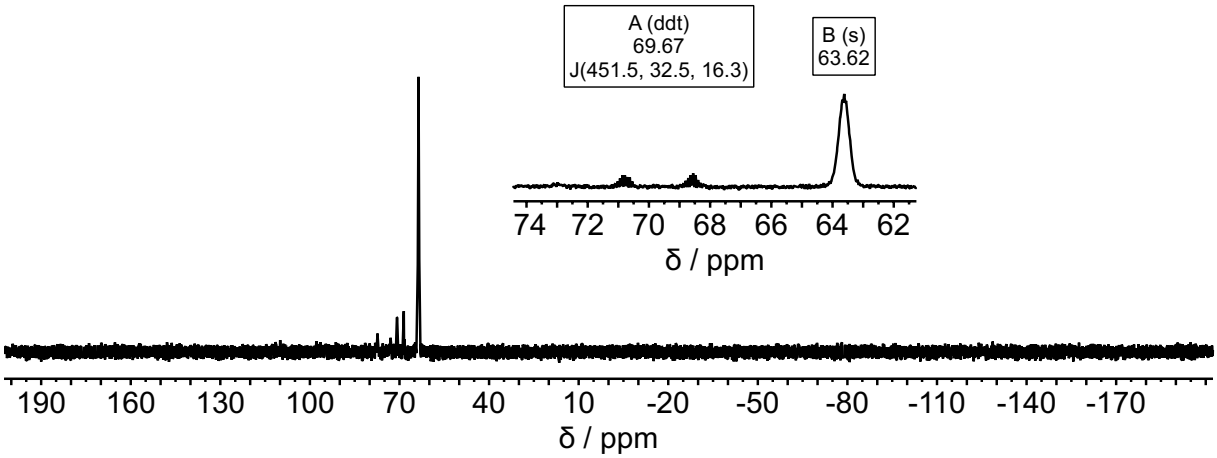

Figure S57. ^{31}P NMR spectrum of Bis$_2$(Cl)Ga–O–P(Bn)^{t}Bu$_2$ (**11**) in C$_6$D$_6$ (202 MHz, 298K).

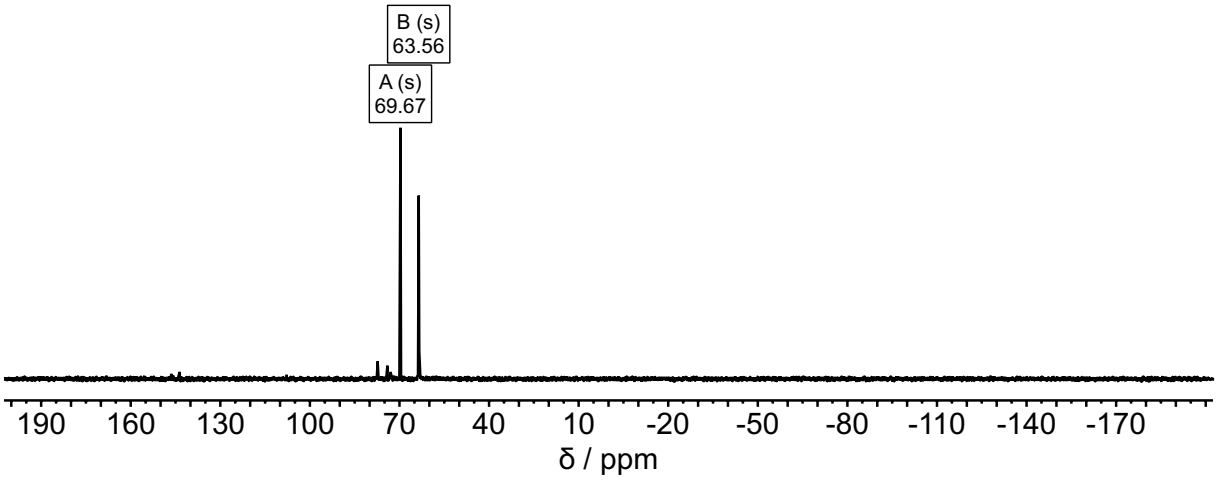

Figure S58. ^{31}P{^{1}H} NMR spectrum of Bis$_2$(Cl)Ga–O–P(Bn)^{t}Bu$_2$ (**11**) in C$_6$D$_6$ (202 MHz, 298K).

3) Crystallographic data

Single crystals were examined on a Rigaku Supernova diffractometer. The crystals were kept at 100.0(1) K during data collection. Using Olex2[3], the structures were solved with the ShelXT[4] structure solution program using Intrinsic Phasing. **1**, **7**, **8**, **9a**, and **10a** were refined with the ShelXL[5] refinement package using least squares minimization, **2** and **11** were refined with olex2.refine 1.5-ac7-020[6]. For **3** the structure was refined with the olex2.refine[6] refinement package using Gauss-Newton minimisation and NoSphereA2,[7] an implementation of NOn-SPHERical Atom-form-factors in Olex2. The following options were used: SOFTWARE: ORCA 5.0 PARTITIONING: NoSpherA2, INT ACCURACY: Normal, METHOD: R2SCAN, PBE BASIS SET: def2-TZVPP, CHARGE: 0, MULTIPLICITY: 1.

Details of the X-ray diffraction investigations are given in Tables S1–S2. CCDC 2528994 – 2529001 contain the supplementary crystallographic data for this paper. These data can be obtained free of charge from The Cambridge Crystallographic Data Centre via www.ccdc.cam.ac.uk/conts/retrieving.html.

Table S1. Crystallographic data for compounds.

Compound	**1**	**2**	**3**	**7**
Empirical formula	$C_{29}H_{62}GaO_2PSi_4$	$C_{27}H_{64}GaO_2PSi_4$	$C_{26}H_{62}GaO_3PSi_4$	$C_{24}H_{60}GaO_2PSi_4$
M [g mol^{-1}]	655.83	633.85	635.819	593.77
T [K]	100.0(1)	100.0(1)	100.00(10)	100.0(1)
λ [Å]	1.54184 (Cu Kα)	0.71073 (Mo Kα)	1.54184 (Cu Kα)	1.54184 (Cu Kα)
Crystal size	0.14×0.08×0.04	0.26×0.19×0.09	0.27×0.17×0.06	0.6×0.23×0.17
Crystal system	orthorhombic	monoclinic	monoclinic	triclinic
Space group	$Pna2_1$	$P2_1/n$	$P2_1/n$	$P\overline{1}$
a [Å]	15.6230(2)	9.6127(3)	9.4833(1)	11.8309(2)
b [Å]	13.7874(1)	17.7417(6)	17.3313(3)	12.0464(2)
c [Å]	17.4384(3)	21.6477(6)	21.9273(3)	12.6821(2)
α [°]	90	90	90	93.784(1)
β [°]	90	93.347(3)	96.632(1)	103.971(1)
γ [°]	90	90	90	96.028(1)
Volume [Å^3]	3756.24(9)	3685.6(2)	3579.81(9)	1736.45(5)
Z	4	4	4	2
ρ_{calc} [g cm^{-3}]	1.160	1.142	1.180	1.136
μ [mm^{-1}]	2.791	0.940	2.932	2.966
F(000) [e]	1416.0	1379.4	1378.9	644.0
2θ range [°]	8.176–152.09	6.604–57.4	6.52–152.84	7.216–151.708
Index ranges	−19 ≤ h ≤ 19 −17 ≤ k ≤ 17 −21 ≤ l ≤ 18	−16 ≤ h ≤ 16 −29 ≤ k ≤ 30 −36 ≤ l ≤ 36	−11 ≤ h ≤ 11 −21 ≤ k ≤ 21 −27 ≤ l ≤ 21	−14 ≤ h ≤ 13 −15 ≤ k ≤ 15 −15 ≤ l ≤ 15
Refl. collected	66533	135646	18112	36117
Independent refl.	7302	9491	7366	7164
R_{int} / R_{sigma}	0.0339/0.0164	0.1041/0.0794	0.0209/0.0249	0.0268/0.0168
Refl. [$I > 2\sigma(I)$]	6604	7589	6758	7017
Data / restraints / parameters	7302/1159/643	9491/0/334	7366/0/502	7164/0/307
GooF on F^2	1.024	1.025	1.064	1.075
R_1 / wR_2 [$I > 2\sigma(I)$]	0.0419/0.1065	0.0316/0.0725	0.0192/0.0425	0.0238/0.0633
R_{int} (all data) / wR_2	0.0467/0.1114	0.0456/0.0783	0.0222/0.0439	0.0243/0.0636
ρ_{fin} (max/min) [e Å^{-3}]	0.28/−0.67	0.55/−0.40	0.19/−0.26	0.42/−0.39
Flack parameter	0.50(7)	–	–	–
CCDC	2528994	2528995	2528996	2528997

1: Refined as a racemic twin with 50:50 distribution. Disorder of the hole molecule over two sites in ratio 50:50 except P3, O1, Ga1, and C5. Model has Chirality at C23A (Polar SPGR) S and at C23B (Polar SPGR) R.

Table S2. Crystallographic data for compounds.

Compound	**8**	**9a**	**10a**	**11**
Empirical formula	$C_{31}H_{68}GaO_2PSi_4$	$C_{30}H_{62}GaOPSi_4$	$C_{27}H_{66}GaOPSi_5$	$C_{29}H_{63}ClGaOPSi_4$
M [g mol^{-1}]	685.90	651.84	647.93	676.31
T [K]	100.0(1)	100.0(2)	100.00(10)	100.0(2)
λ [Å]	0.71073 (Mo Kα)	0.71073 (Mo Kα)	0.71073 (Mo Kα)	0.71073 (Mo Kα)
Crystal size	0.36×0.19×0.04	0.36×0.2×0.08	0.36×0.29×0.03	0.35×0.14×0.09
Crystal system	triclinic	triclinic	monoclinic	monoclinic
Space group	$P\bar{1}$	$P\bar{1}$	$P2_1/c$	$P2_1/n$
a [Å]	11.9851(4)	11.1921(2)	18.0341(4)	9.5943(4)
b [Å]	12.0145(4)	18.7628(2)	12.4971(3)	34.9093(11)
c [Å]	15.2010(6)	19.2984(3)	17.9023(3)	12.2714(4)
α [°]	109.461(3)	76.878(1)	90	90
β [°]	96.402(3)	75.437(1)	103.1506(19)	112.201(4)
γ [°]	94.595(3)	89.215(1)	90	90
Volume [Å^3]	2034.82(13)	3815.9(1)	3928.90(14)	3805.4(3)
Z	2	4	4	4
ρ_{calc} [g cm^{-3}]	1.119	1.135	1.095	1.180
μ [mm^{-1}]	0.856	0.908	0.911	0.981
F(000) [e]	744.0	1408.0	1408.0	1460.0
2θ range [°]	6.81–52.044	6.55–56.566	6.52–65.228	6.54–56.4
Index ranges	−14 ≤ h ≤ 14, −14 ≤ k ≤ 14, −18 ≤ l ≤ 18	−14 ≤ h ≤ 14, −25 ≤ k ≤ 25, −25 ≤ l ≤ 25	−27 ≤ h ≤ 26, −18 ≤ k ≤ 18, −26 ≤ l ≤ 27	−14 ≤ h ≤ 13, −50 ≤ k ≤ 50, −18 ≤ l ≤ 18
Refl. collected	42468	216908	167447	98762
Independent refl.	8004	18876	13910	9811
R_{int} / R_{sigma}	0.0377/0.0278	0.0639/0.0293	0.0634/0.0284	0.0894/0.0787
Refl. [$I > 2\sigma(I)$]	6869	15831	11935	7912
Data / restraints / parameters	8004/397/401	18876/0/711	13910/309/425	9811/2/392
GooF on F^2	1.037	1.044	1.095	1.056
R_1 / wR_2 [$I > 2\sigma(I)$]	0.0456/0.1083	0.0310/0.0734	0.0370/0.0820	0.0487/0.0879
R_{int} (all data) / wR_2	0.0541/0.1134	0.0417/0.0778	0.0478/0.0863	0.0669/0.0940
ρ_{fin} (max/min) [e Å^{-3}]	0.99/−0.52	0.52/−0.35	0.67/−0.78	0.66/−0.67
CCDC	2528998	2528999	2529000	2529001

8: The unit cell contains heavily disordered benzene solvent molecules. Therefore, a solvent mask was calculated, and 72 electrons were found in a volume of 401Å^3 in 1 void per unit cell. This is consistent with the presence of one benzene solvent molecule per Asymmetric Unit which account for 84 electrons

per unit cell. The main molecules is seriously disordered, suitable restraints (SIMU, RIGU SADI) were applied, the thermal motion of the minor occupied atoms were refined isotropically; **10a**: Disorder of C17, C18, C20 and C22 over two sites in a ratio of 61:39, and of Si5, C25 to C27 over two sites in a ratio of 70:30. Necessary restraints (SIMU, RIGU and SADI for the disordered atoms) and one constraint (EADP for C15A and C15B) were applied. The hydrogen atom bonded to P1 was refined isotropically; **11**: Rotational disorder of one trimethylsilyl group (C2-4) and disorder of the Cl substituent over two sites; ratio 58:42.

4) Quantum-chemical calculations

Calculations have been performed using Orca 6.0.1 software package,[8] unless otherwise stated. Molecular structures of selected studied compounds have been optimised at the PBEh-3c level of theory[9] using restricted Kohn-Sham (RKS) formalism. All species were modelled as isolated molecules. As starting approximations, the geometries from the available experimental crystal structures were taken. Otherwise, they were modelled manually. The target convergence in geometry optimisations has been set to *TightOpt*. Also, in all calculations we used the settings *TightSCF* and *DefGrid3*, as well as the RIJCOSX accelerating approximation.[10] The obtained molecular structures are shown in Figures S59 – S62. The obtained relative energies are collected in Tables S3 and S4. For obtaining the Gibbs free energies ΔG^0_{298}, harmonic frequencies were calculated analytically. These were used in statistical thermodynamic computations applying the Quasi-RRHO approximation[11] with standard settings as implemented in Orca.

Table S3. Relative electronic (ΔE) and Gibbs free energies (ΔG^0_{298}) for **GaOP**·PhC≡CH (**9**).

Reaction	ΔE [kcal mol^{-1}]	ΔG^0_{298} [kcal mol^{-1}]
Deprotonation product **GaOP**·PhC≡CH **9a**	26.6	22.0
Ring-closure product **GaOP**·PhC≡CH **9b**	0	0

Table S4. Relative electronic (ΔE) and Gibbs free energies (ΔG^0_{298}) for **GaOP**·Me_3SiC≡CH (**10**).

Reaction	ΔE [kcal mol^{-1}]	ΔG^0_{298} [kcal mol^{-1}]
Deprotonation product **GaOP**·Me_3SiC≡CH **10a**	14.8	8.9
Ring-closure product **GaOP**·Me_3SiC≡CH **10b**	0	0

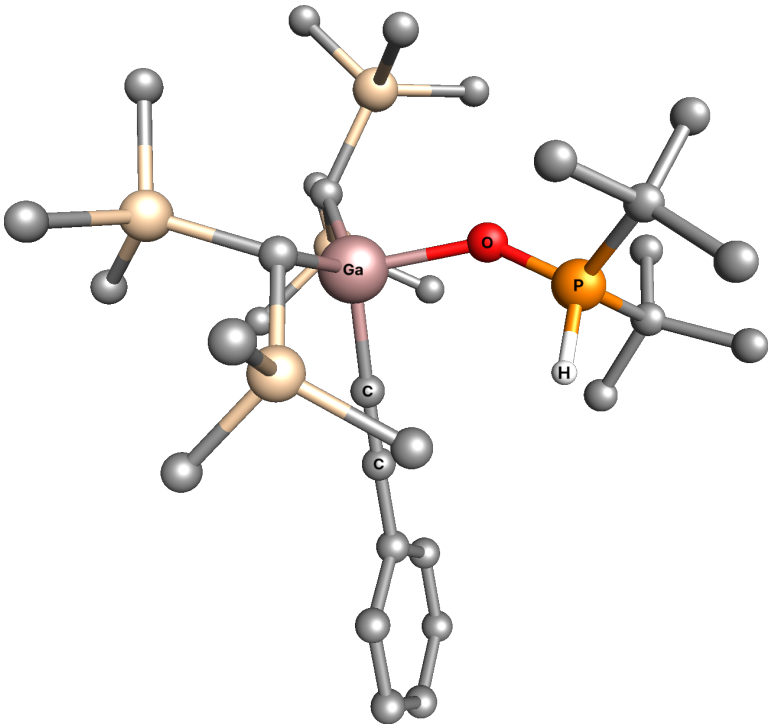

Figure S59. Optimised molecular structure of deprotonation product **GaOP**·PhC≡CH (**9a**). (RKS-PBEh-3c). Hydrogen atoms are omitted for clarity.

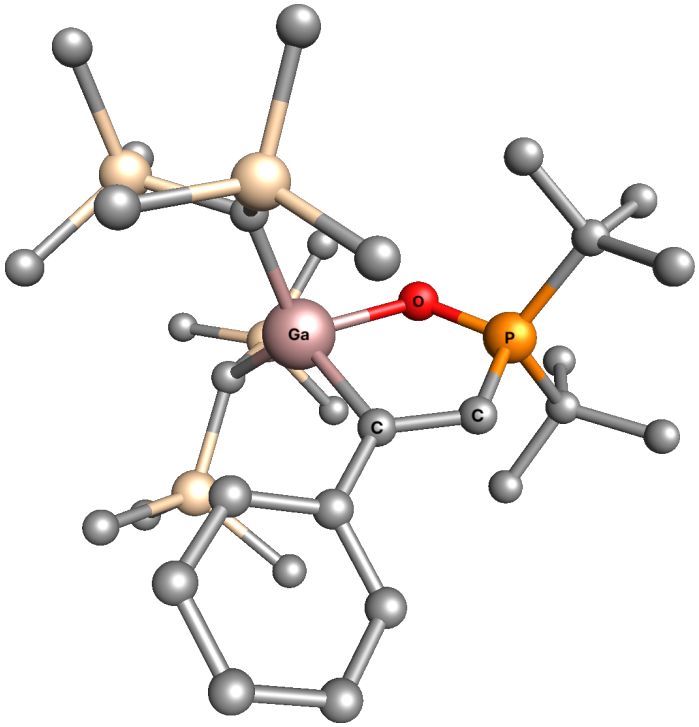

Figure S60. Optimised molecular structure of ring-closure product **GaOP**·PhC≡CH (**9b**). (RKS-PBEh-3c). Hydrogen atoms are omitted for clarity.

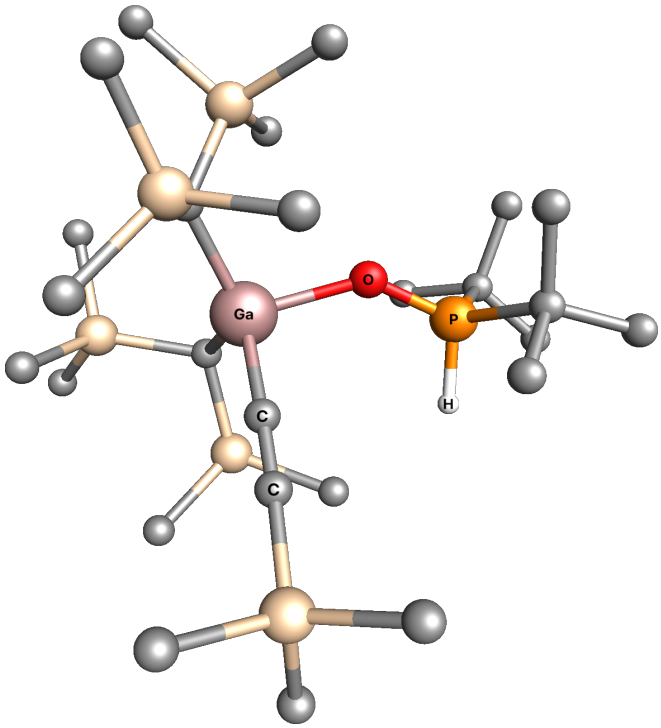

Figure S61. Optimised molecular structure of deprotonation product **GaOP**·$Me_3SiC{\equiv}CH$ (**10a**). (RKS-PBEh-3c). Hydrogen atoms are omitted for clarity.

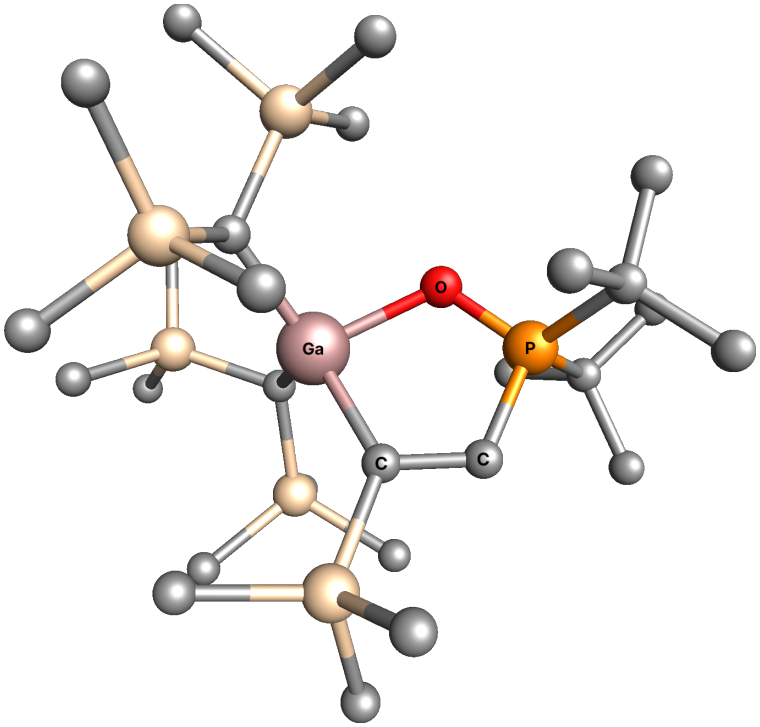

Figure S62. Optimised molecular structure of ring-closure product **GaOP**·$Me_3SiC{\equiv}CH$ (**10b**). (RKS-PBEh-3c). Hydrogen atoms are omitted for clarity.

5) Proposed mechanisms

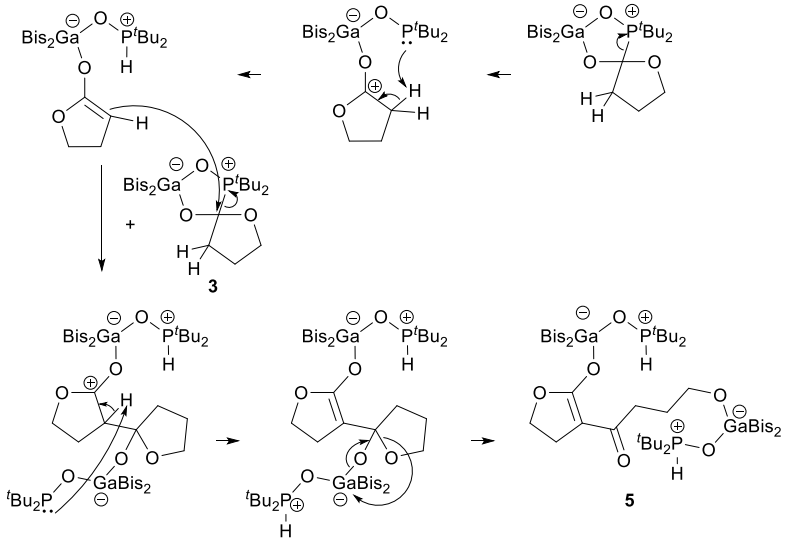

Scheme S1. Proposed mechanism for the *γ*-butyrolactone rearrangement of the $Bis_2Ga–O–P^tBu_2$ FLP.

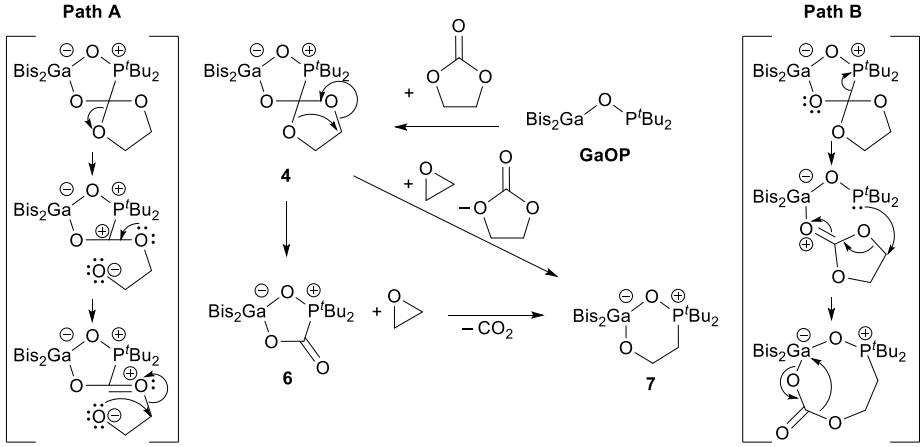

Scheme S2. Proposed mechanism for the ethylene carbonate splitting of the $Bis_2Ga–O–P^tBu_2$ FLP.

6) References

1 J. Buth, M. J. Klingsiek, Y. V. Vishnevskiy, A. Mix, J.-H. Lamm, B. Neumann, H.-G. Stammler and N. W. Mitzel, *ChemistryEurope*, 2026, **4**, e202500307.

2 J. Buth, Y. V. Vishnevskiy, J.-H. Lamm, B. Neumann, H.-G. Stammler and N. W. Mitzel, *Dalton Trans.*, 2026, **55**, 2691–2701.

3 O. V. Dolomanov, L. J. Bourhis, R. J. Gildea, J. A. K. Howard and H. Puschmann, *J. Appl. Crystallogr.*, 2009, **42**, 339–341.

4 G. M. Sheldrick, *Acta Crystallogr., Sect. A:Found. Adv.*, 2015, **71**, 3–8.

5 G. M. Sheldrick, *Acta Crystallogr., Sect. C:Struct. Chem.*, 2015, **71**, 3–8.

6 L. J. Bourhis, O. V. Dolomanov, R. J. Gildea, J. A. K. Howard and H. Puschmann, *Acta Crystallogr., Sect. A:Found. Adv.*, 2015, **71**, 59–75.

7 F. Kleemiss, O. V. Dolomanov, M. Bodensteiner, N. Peyerimhoff, L. Midgley, L. J. Bourhis, A. Genoni, L. A. Malaspina, D. Jayatilaka, J. L. Spencer, F. White, B. Grundkötter-Stock, S. Steinhauer, D. Lentz, H. Puschmann and S. Grabowsky, *Chem. Sci.*, 2021, **12**, 1675–1692.

8 F. Neese, *WIREs Comput. Mol. Sci.*, 2022, **12**, e1606.

9 S. Grimme, J. G. Brandenburg, C. Bannwarth and A. Hansen, *J. Chem. Phys.*, 2015, **143**, 054107.

10 F. Neese, F. Wennmohs, A. Hansen and U. Becker, *Chem. Phys.*, 2009, **356**, 98–109.

11 S. Grimme, *Chem.–Eur. J.*, 2012, **18**, 9955–9964.